Journal of Materials Chemistry B

Accepted Manuscript

ROYAL SOCIETY OF CHEMISTRY

www.rsc.org/materialsB

New Application of Fluorescent Organotin Compounds Derived from Schiff Bases: Synthesis, X-ray Structures, Photophysical Properties, Cytotoxicity and Fluorescent Bioimaging†

Víctor M. Jiménez-Pérez,[a,*] María C. García-López,[a] Blanca M. Muñoz-Flores,[a] Rodrigo Chan-Navarro,[a] Jessica Berrones,[a] H. V. Rasika Dias,[b] Ivana Moggio,[c] Eduardo Arias,[c] Jesús A. Serrano,[d] and Arturo Chavez-Reyes.[d,*]

[a] Universidad Autónoma de Nuevo León, Facultad de Ciencias Químicas, Ciudad Universitaria, Av. Universidad s/n. C. P. 66451, Nuevo León, México.

[b] Department of Chemistry and Biochemistry, The University of Texas at Arlington, Arlington Texas, 76019-0065, USA.

[c] Centro de Investigación en Química Aplicada, Boulevard Enrique Reyna 140, 25294 Saltillo, México.

[d] Centro de Investigación y de Estudios Avanzados del IPN, Unidad Monterrey, PIIT, C.P. 66600. Apodaca, Nuevo León, México.

Key words: Fluorescent bioimaging, organotin, quantum yield, X-ray, ^{119}Sn-NMR, confocal microscopy.

* E-mail: vjimenezpr@uanl.edu.mx (V. M. J. P.), achavez@cinvestav.mx (A. C. R.)

This paper is dedicated to Professor José Norberto Farfán García on his 60th birthday

† Electronic supplementary information (ESI) available: The details of ^{1}H, ^{13}C, ^{119}Sn NMR (2D experiments), absorption and emission spectra. TOF MS, IR are included. See DOI:

Abstract

A series of eight new organotin compounds derived from Schiff bases has been prepared by multicomponent reaction from 2-hydroxy-1-naphthaldehyde or 4-substituted-2-hydroxybenzalhedyde, benzhydrazine, and the corresponding diorganotin oxide (R_2SnO, R = ^{n}Bu or Ph). All of the compounds were fully characterized by NMR (^{1}H, ^{13}C, and ^{119}Sn), IR, UV/Vis, elemental analyses and fluorescence spectroscopy. The crystal structures for some organotin compounds were determined by single crystal X-ray diffraction analysis. All of the compounds display fluorescence at room temperature with quantum yields of about 2 x 10^{-4} to 0.56. The cytotoxic activity and cellular imaging studies were carried out with the newly synthesized compounds. To the best of our knowledge, this is the first report of organotin compounds with Schiff base ligands investigated for fluorescence bioimaging (FBI).

1. Introduction

Fluorescence bioimaging (FBI) has been of great importance in biomedical, biological and related sciences in recent years, because it is the unique imaging technology with which it is possible to visualize morphological details in tissue at subcellular resolution by confocal microscopy, while radiography, ultrasound, magnetic resonance imaging (MRI), and X-ray computed tomography (CT) have not been able to accomplish.[1]

In imaging analysis, it is important to include counter stain dies in order to have structural references to help with the images interpretation. There are several fluorochromes that bind to DNA and stain the nucleus of the cells. Such compounds are very useful when cytoplasmic structures are studied. However, when nuclear structures are of interest, such compounds could interfere and make the analysis difficult. For these cases, a cytoplasm counter stain die would work better. Therefore, the design and synthesis of new potential fluorescent imaging agents have become a dynamic research field, where the organometallic compounds have played a notable role.[2,3] Recently, it has been reported that tridentate Schiff bases can act as analytical fluorescent chemosensors for metal identification in live cell by confocal microscopy.[4,5,6]

In the last few years, novel organotin compounds derived from Schiff bases have shown interesting properties such as luminescence.[7,8] Indeed, a potential application of fluorescent organotin compounds in organic light emitting diode (OLED) fabrication has been reported.[9,10] Although some luminescent organotin derivatives have been researched,[11,12] (chart 1, **I**-**IX**) the bioimaging studies have not been reported yet. To this respect, we are interested in the preparation of organotin compounds derived from ligands with electrodonor atoms, such as nitrogen and oxygen[13,14] as well as their biological activity.[15,16] Thus, we are reporting the new application of eight organotin compounds derived from 1-hydroxynaphthylbenzhydrazine. All of the organotin compounds were fully characterized by spectroscopic and spectrometric methods. The elucidation of molecular structures for some of them by X-ray diffraction is reported. The cytotoxic activity and the application in bioimaging cells of the organotin compounds were tested.

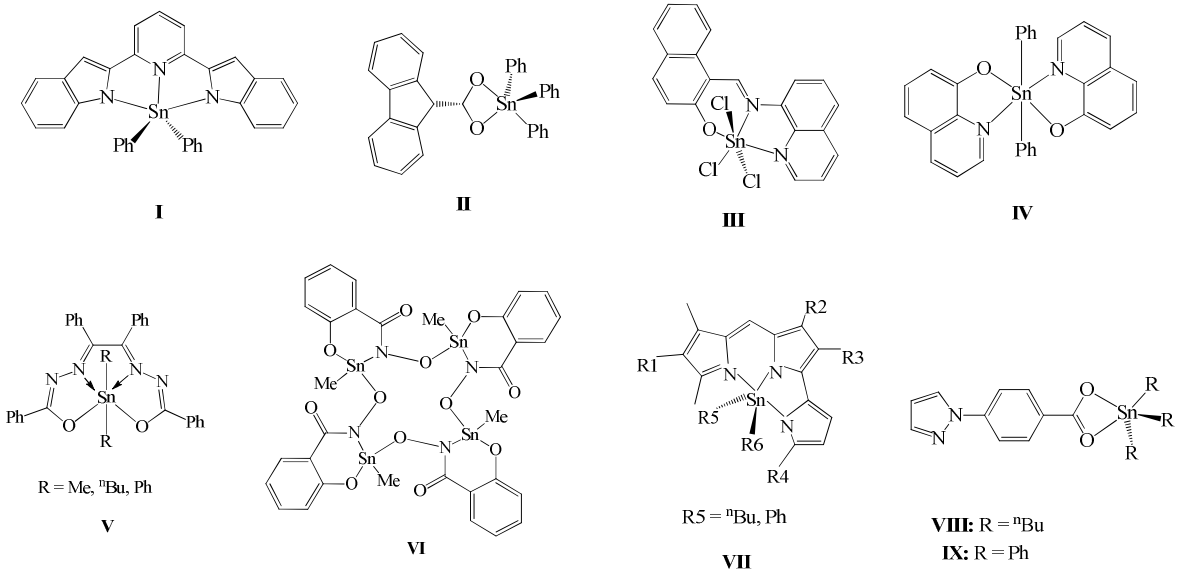

Chart 1 Luminescent organotin compounds.

2. Experimental section

2.1. General remarks

All the manipulations were performed under dried nitrogen in standard Schlenk glassware.[17] All starting materials were purchased from Aldrich Chemical Company. Solvents were used without further purification. Melting point tests were carried out on an Electrothermal Mel-Temp apparatus and are uncorrected. Infrared spectra were recorded using a Bruker Tensor 27 FT-IR spectrophotometer, equipped with a Pike Miracle ™ ATR accessory with single reflection ZnSe ATR crystal. High resolution mass spectra were acquired by LC/MSD TOF on an Agilent Technologies instrument with APCI as ionization source. ^{1}H, ^{13}C and ^{119}Sn-NMR spectra were recorded in $CDCl_3$ and $(CD_3)_2SO$ on a Bruker advance DPX 400: ^{1}H (399.78 MHz), ^{13}C (100.52 MHz) and ^{119}Sn (149.4 MHz). Chemical shifts (ppm) are relative to $(CH_3)_4Si$ for ^{1}H and ^{13}C and to $(CH_3)_4Sn$ for ^{119}Sn.

2.2. General procedure of multicomponent reactions to organotin complexes 1-8

[N-(2-oxido-1-naphthaldehyde)-4-nitrobenzyhydrazidato] di-*n*-butyltin(IV) **1**

A solution of 2-hydroxynaphtaldehyde (0.68, 4 mmol), 4-nitro-benzoylhydrazine (0.72 g, 4 mmol), and di-*n*-butyltin oxide (0.99 g, 4 mmol) in benzene (50 mL) was heated to reflux for 20 h in a Dean-Stark tramp for the azeotropic removal of water, and allowed to cool to room temperature. Then, all volatiles were removed under vacuum. The residue was extracted with toluene to yield **1** as red-deep solid (1.86 g, yield: 91 %). M. p. 139 °C. ^{1}H-NMR (400.13 MHz, $CDCl_3$, 298 K) δ: 0.87 (t, 6H, ^{3}J = 7.2 Hz, CH_3-δ), 1.39 (m, 4H, ^{3}J = 7.2 Hz, CH_2-γ), 1.58 (t, 4H, ^{3}J = 7.2 Hz, CH_2-α), 1.65 (m, 4H, ^{3}J = 7.2 Hz, CH_2-β), 6.94 (d, 1H, ^{3}J = 9.2 Hz, H-2), 7.33 (t, 1H, ^{3}J = 7.2 Hz, H-6), 7.54 (t, 1H, ^{3}J = 7.2 Hz, H-7), 7.70 (d, 1H, ^{3}J = 8.0 Hz, H-5), 7.78 (d, 1H, ^{3}J = 9.2 Hz, H-3), 7.97 (d, 2H, ^{3}J = 8.4 Hz, H-14, H-18), 8.07 (d, 1H, ^{3}J = 8.8 Hz, H-8), 8.30 (d, 2H, ^{3}J = 8.4 Hz, H-15, H-17), 9.68 (s, 1H, ^{3}J (^{1}H-^{119}Sn) = 48 Hz, H-11). ^{13}C-NMR (100.61 MHz, $CDCl_3$, 298 K) δ: 13.57 (*C*H_3-δ), 22.26 (*C*H_2-α), 26.42 (*C*H_2-γ), 26.80 (*C*H_2-β), 106.97 (C-10), 119.04 (C-8), 123.25 (C-6), 123.89 (C-15, C-17), 124.35 (C-2), 127.21 (C-4), 128.25 (C-7), 128.55 (C-14, C-18), 129.27 (C-5), 133.78 (C-9), 137.35 (C-3), 139.76 (C-13), 149.09 (C-16), 158.20 (C-11), 166.18 (C-12), 170.01 (C-1). COSY correlation [δ_H/δ_H]: 0.87/1.39 (H-δ/H-γ), 1.39/1.65 (H-γ/H-β), 1.58/1.65 (H-α/H-β), 6.94/7.78 (H-2/H-3), 7.33/7.54 (H-6/H-7), 7.33/7.70 (H-6/H-5), 7.54/8.07 (H-7/H-8), 7.97/8.3 (H14, H-18/H-15, H-17). HSQC correlation [δ_H/δ_C]: 0.85/13.5 (H-δ/C-δ), 1.39/26.4 (H-γ/C-γ), 1.58/22.2 (H-α/C-α), 1.65/26.8 (H-β/C-β),

6.94/124.35 (H-2/C-2), 7.33/123.2 (H-6/C-6), 7.54/128.2 (H-7/C-7), 7.7/129.2 (H-5/C-5), 7.78/137.3 (H-3/C-3), 7.97/128.5 (H-14,H-18/C-14,C-18), 8.07/119 (H-8/C-8), 8.3/123.8 (H-15,H-17/C-15,C-16). HMBC correlation [δ_H/δ_C]: 0.85/26.4,26.8 (H-δ/C-γ,C-β), 1.39/ 13.5, 22.2 (H-γ/C-δ,C-α), 1.58/ 26.2, 26.8 (H-α/C-γ,C-β), 1.65/22.2,26.4 (H-β/C-α,C-γ), 6.94/106.9,127.2,170 (H-2/C-10,C-4,C-1), 7.33/119,127.2, (H-6/C-8,C-4), 7.54/129.2,133.7 (H-7/C-5,C-9), 7.7/128.2,133.7, (H-5/C-4,C-9), 7.78/127.2,133.7,170 (H-3/C-4,C-9,C-1), 7.97/149,166.1, (H-14,H-18/C-16,C-12), 8.07/106.9,127.2, (H-8/C-10,C-4), 8.3/139.7,149,166.1 (H-15,H-16/C-13,C-16,C-12), 9.68/106.9,133.7,170 (H-11/C-10,C-9,C-1). ^{119}Sn-NMR (149 MHz, $CDCl_3$, 298 K) δ: - 246.93 ppm. IR (ATR) $\tilde{\nu}_{max}$ (cm^{-1}): 2959, 2920, 2854 (C-$H_{n\text{-}Bu}$), 1597, 1582, 1525, 1454, 1395, 1336, 1190, 1144, 1104, 967, 846, 822, 747, 710. UV/Vis: λ_{max} (nm) = 457 (THF, $1x10^{-3}$ M), 460 ($CHCl_3$, $1x10^{-3}$ M). Anal. calcd. for $C_{26}H_{29}N_3O_4Sn$: C 55.15 %, H 5.16 %, N 7.42 %; Found: C 55.48 %, H 5.36 %, N 7.45 %.

[N-(2-oxido-1-naphthaldehyde)-4-nitrobenzyhydrazidato] diphenyltin(IV) **2**

The procedure was similar to the synthesis of **1**. Orange solid (88 %). M. p. 279 °C. ^{1}H NMR (400.13 MHz, $CDCl_3$, 298 K) δ: 7.27 (d, 1H, ^3J = 10 Hz, H-2), 7.36 (t, 1H, ^3J = 7.6 Hz, H-6), 7.44 (m, 6H, ^3J = 4 Hz, H-*m*, H-*p*), 7.55 (t, 1H, ^3J = 7.6 Hz, H-7), 7.74 (d, 1H, ^3J = 8.0 Hz, H-5), 7.89 (d, 4H, $^3J(^{119}Sn\text{-}^1H)$ = 65 Hz, H-*o*), 7.9 (d, 1H, ^3J = 10.8 Hz, H-3), 8.06 (d, 1H, ^3J = 8.4 Hz, H-8), 8.32 (d, 2H, ^3J = 8.4 Hz, H-15, H-17), 8.41 (d, 2H, ^3J = 8.8 Hz, H-14, H-18), 9.71 (s, 1H, $^3J(^{119}Sn\text{-}^1H)$ = 62 Hz, H-11). ^{13}C NMR (100.61 MHz, $CDCl_3$, 298 K) δ: 107.33 (C-10), 119.15 (C-8), 123.49 (C-15, C-17), 123.62 (C-6), 124.35 (C-2), 127.46 (C-4), 128.48 (C-14, C-18, C-7), 129.02 (C-γ), 129.34 (C-5), 130.73 (C-7), 133.67 (C-9), 135.98 (C-β), 137.93 (C-3), 138.57 (C-α), 139.36 (C-13), 149.26 (C-16), 158.46 (C-11), 165.87 (C-12), 170.25 (C-1). COSY correlation [δ_H/δ_H]: 7.27/7.90 (H-2/H-3), 7.36/7.55 (H-6/H-7), 7.36/7.74 (H-6/H-5), 7.43-7.44/7.86-7.88 (H-γ/H-β), 7.55/8.06 (H-7/H-8), 8.32/8.41 (H-15, H-17/ H-14, H-18), HSQC correlation [δ_H/δ_C]: 7.27/124.35 (H-2/C-2), 7.36/123.62 (H-6/C-6), 7.43-7.44/ 129.02, 130.73 (H-γ, H-δ/C-γ, C-δ), 7.55/128.48 (H-7/C-7), 7.74/129.34 (H-5/C-5), 7.86-7.88/135.98 (H-β/C-β), 7.90/137.93 (H-3/C-3), 8.06/119.15 (H-8/C-8), 8.32/123.49 (H-15, H-17/ C-15, C-17), 8.41/128.48 (H-14, H-18/ C-14, C-18), HMBC correlation [δ_H/δ_C]: 7.27/107.33, 127.46, 170. 25 (H-2/C-10, C-4, C-

1), 7.36/119.15, 127.5, 128.48, 129.34 (H-6/C-8, C-4, C-7, C-5), 7.43-7.44/ 138.57, 129.02 (H-γ, H-δ/ C-α,C-γ), 7.55/129.34, 133.67 (H-7/ C-5, C-9), 7.74/127.46, 128.48, 133.67, 137.93, (H-5/C-4, C-7, C-9, C-3), 7.86-7.88/129.02, 130.73,138.57 (H-β/C-γ, C-δ, C-α), 7.90/127.46, 129.34, 133.67, 170.25 (H-3/ C-4, C-5, C-9, C-1), 8.06/107.33, 123.62, 127.46, 128.48, 133.67 (H-8/C-10, C-6, C-4, C-7, C-9), 8.32/139.36, 149.34 (H-15, H-17/ C-13, C-16), 8.41/149.34, 165.87 (H-14, H-15/ C-16, C-12). ^{119}Sn NMR (149 MHz, $CDCl_3$, 298 K) δ: - 327.18 ppm. IR (ATR) $\tilde{\nu}_{max}$ (cm^{-1}): 3036, 1596 (C-O), 1589, 1525, 1454, 1429, 1392, 1336, 1193, 1142, 970, 862, 834, 753, 732, 713. UV/Vis: λ_{max} (nm) = 475 (THF, $1x10^{-3}$ M), 477 ($CHCl_3$, $1x10^{-3}$ M). Anal. calcd. for $C_{30}H_{21}N_3O_4Sn$: C 59.44 %, H 3.49 %, N 6.93 %; Found: C 59.42 %, H 3.57 %, N 6.57 %.

[N-(2-oxido-1-naphthaldehyde)-benzyhydrazidato] di-n-butyltin(IV) **3**

The procedure was similar to the synthesis of **1** as brown oil (80 %). ^{1}H NMR (400.13 MHz, $CDCl_3$, 298 K) δ: 0.74 (t, 6H, ^3J = 7.2 Hz, CH_3-δ), 1.25 (m, 4H, CH_2-γ), 1.43 (t, 4H, ^3J = 7.2 Hz, CH_2-α), 1.59 (m, 4H, ^3J = 7.2 Hz, CH_2-β), 6.93 (d, 1H, ^3J = 9.2 Hz, H-2), 7.26 (t, 1H, ^3J = 7.6 Hz, H-6), 7.43, (m, 3H, H-15-17), 7.47 (t, 1H, ^3J = 7.6 Hz, H-7), 7.63 (d, 1H, ^3J = 8.0 Hz, H-5), 7.71 (d, 1H, ^3J = 8.8 Hz, H-3), 8.04 (d, 1H, ^3J = 8.4 Hz, H-8), 8.14 (m, 2H, H-14, H-18), 9.60 (s, 1H, ^3J (^{1}H-^{119}Sn) = 48 Hz, H-11). ^{13}C NMR (100.61 MHz, $CDCl_3$, 298 K) δ: 13.69 (Cδ), 22.06 [Cα, ^1J (^{13}C-$^{119/117}$Sn) = 595/568 Hz], 26.54 [Cγ, ^3J (^{13}C-^{119}Sn) = 82 Hz], 26.96 [Cβ, ^2J (^{13}C-^{119}Sn) = 35 Hz], 107.17 (C-9), 119.21 (C-8), 122.85 (C-6), 124.26 (C-2), 127.25 (C-4), 127.44 (C-14,18), 127.8 (C-7), 128.1 (C-15,17), 129.03 (C-5), 130.68 (C-16), 133.54 (C-10), 133.73 (C-13), 136. 41 (C-3), 156.77 [C-11, ^2J (^{13}C-^{119}Sn) = 20 Hz], 168.55 [C-12, ^2J (^{13}C-^{119}Sn) = 10 Hz], 169.42 [C-1, ^2J (^{13}C-^{119}Sn) = 33 Hz]. COSY correlation [δ_H/δ_H]: 6.93/7.71 (H-2/H-3), 7.26/7.47 (H-6/H-7), 7.26/7.63 (H-6/H-5), 7.43/8.14 (H-15/H-14). HETCOR correlation [δ_H/δ_C]: 0.74/13.69 (Hδ/Cδ), 1.25/26.54 (Hγ/Cγ), 1.43/22.06 (Hα/Cα), 1.59/26.96 (Hβ/Cβ), 6.93/124.26 (H-2/C-2), 7.26/122.85 (H-6/C-6), 7.43/128.1 (H-15, H-17/C-15, C-17), 7.47/127.8 (H-7/C-7), 7.63/129.03 (H-5/C-5), 7.71/136.41 (H-3/C-3), 8.04/119.21 (H-8/C-8), 8.14/127.44 (H-14, H-18/C-14, C-18), 9.60/156.77 (H-11/C-11). ^{119}Sn NMR (149 MHz, $CDCl_3$, ppm, 298 K) δ: - 189.99. IR (ATR) $\tilde{\nu}_{max}$ (cm^{-1}): 1598, 1577, 1540, 1508 (C=N). UV/Vis: λ_{max} (nm) = 457

(THF, $1x10^{-3}$ M), 459 ($CHCl_3$, $1x10^{-3}$ M). TOF calc. for [($C_{26}H_{31}N_2O_2Sn+H)^+$] : 523.140203; Found: 523.140324 (error = 0.229467 ppm).

[N-(2-oxido-1-naphthaldehyde)-benzyhydrazidato] diphenyltin(IV) **4**

The procedure was similar to the synthesis of **1** as yellow solid (81 %). M. p. 200 °C. ^{1}H NMR (400.13 MHz, DMSO-d_6, 298 K) δ: 7.19 (d, 1H, ^3J = 9.2 Hz, H-2), 7.31-7.39 (m, 7H, H-6, H-*m*, H-*p*), 7.50-7.55 (m, 4H, H-7,H-15, H-16, H-17), 7.69 (d, 4H, ^3J = 6.4 Hz, H-*o*), 7.81 (1H, d, ^3J = 8.0 Hz, H-5), 7.94 (1H, d, ^3J = 9.2 Hz, H-3), 8.19 (2H, d, ^3J = 7.6 Hz, H-14, H-18), 8.26 (1H, d, ^3J = 8.4 Hz, H-8), 9.59 (s, 1H, ^3J (^{1}H-^{119}Sn) = 52 Hz, H-11). ^{13}C NMR (100.61 MHz, DMSO-d_6, 298 K) δ: 107.51 (C-10), 119.97 (C-8), 123.06 (C-6), 124.48 (C-2), 126.85 (C-4), 127.27 (C-14,18), 128.02 (C-7), 128.40 (C-15,17), 128.47 (C-γ), 128.91 (C-5), 129.04 [C-*m*, ^3J (^{13}C-^{119}Sn) = 86 Hz], 130.67 [C-16, ^3J (^{13}C-^{119}Sn) = 18 Hz], 133.28 (C-9), 133.42 (C-13), 136.25 [C-*o*, ^2J (^{13}C-^{119}Sn) = 55 Hz], 137.2 (C-3), 139.12 [C-*i*, ^1J (^{13}C-$^{119/117}$Sn) = 982/942 Hz], 157.28 (C-11), 168.27 (C-12), 169.64 (C-1). COSY correlation [δ_H/δ_H]: 7.19/7.94 (H-2/H-3), 7.31-7.39 (H-γ/H-β), 7.31-7.39 (H-6/H-5), 7.50-7.55 (H-7/H-8), 7.50-7.55/8.19 (H-15, H-17/ H-14, H-18). ^{119}Sn NMR (149 MHz, DMSO-d_6, 298 K) δ: - 406.72 ppm. IR (ATR) $\tilde{\nu}_{max}$ (cm^{-1}): 3049, 1599, 1574, 1537, 1509, 1429 (C=N), 1392, 1336, 1190, 1144, 967, 818, 750, 710. UV/Vis: λ_{max} (nm) = 457 (THF, $1x10^{-3}$ M), 459 ($CHCl_3$, $1x10^{-3}$ M). Anal. calcd. for $C_{30}H_{22}N_2O_2Sn$: C 64.20 %, H 3.95 %, N 4.99 %; Found: C 64.14 %, H 4.10 %, N 4.72 %.

[N-(4-diethylamino-2-oxidobenzylidene)-4-nitrobenzyhydrazidato] di-n-butyltin(IV) **5**

The procedure was similar to the synthesis of **1** as red solid (81%). M. p. 132 °C. ^{1}H NMR (400 MHz, $CDCl_3$, 298 K): δ 0.86 (t, 6H, *J* = 7.2 Hz, H-δ), 1.20 (t, 6H, *J* = 7.2 Hz, H-16,18), 1.36 (sx, 4H, *J* = 7.6 Hz, H-γ), 1.50 (m, 4H, ^2J (^{119}Sn,^{1}H) = 88 Hz, H-α), 1.66 (m, 4H, H-β), 3.39 (q, 4H, *J* = 6.8, 12 Hz, H-15,17), 5.94 (d, 1H, *J* = 2.0 Hz, H-2), 6.16 (dd, 1H, *J* = 2.0, 8.8 Hz, H-4), 6.96 (d, 1H, *J* = 9.2 Hz, H-5), 8.18(d, 2H, *J* = 9.2 Hz, H-10,14), 8.23 (d, 2H, *J* = 9.2 Hz, H-11,13), 8.49 (s, 1H, ^2J(^{119}Sn,^{1}H) = 46 Hz, H-7). ^{13}C NMR (100 MHz, $CDCl_3$, 298 K): δ 12.94 (C-16,18), 13.72 (C-δ), 22.14 (C-α, ^1J($^{119/117}$Sn,^{13}C) = 603/577 Hz), 26.55 (C-γ, ^3J(^{119}Sn,^{13}C) = 84 Hz), 27.01 (C-β, ^2J(^{119}Sn,^{13}C) = 35 Hz), 44.56 (C-15,17), 100.55 (C-2), 104.01 (C-4), 107.13 (C-6), 123.38 (C-11,13), 128.10 (C-10,14),

136.60 (C-5), 140.49 (C-9), 148.82 (C-12), 154.24 (C-3), 160.96 (C-7, $^{2}J(^{119}Sn,^{13}C)$ = 22 Hz), 165.02 (C-1), 169.27 (C-8, $^{2}J(^{119}Sn,^{13}C)$ = 31 Hz). HETCOR correlation [δ_H/δ_C]: 0.86/13.72 (H-δ/C- δ), 1.20/12.94 (H-16,18/C-16,18), 1.36/26.55 (H-γ/C-γ), 1.50/22.14 (H-α/C-α), 3.39/44.72 (H-15,17/C-15,17), 5.94/100.55 (H-2/C-2), 6.16/104.01 (H-4/C-4), 6.96/136.60 (H-5/C-5), 8.18/128.10 (H-10,14/C-10,14), 8.23/123.38 (H-11,13/C-11,13), 8.49/160.96 (H-7/C-7). COSY correlation [δ_H/δ_H]: 1.20/3.39 (H-16,18/H-15,17), 1.36/1.66 (H-γ/H-β), 1.50/0.87 (H-α/H-β), 1.36/0.86 (H-γ/H-δ), 6.16/5.94 (H-4/H-2), 6.96/6.16 (H-5/H-4), 8.18/8.23 (H-10,14/H-11,13). ^{119}Sn NMR (128 MHz, $CDCl_3$): δ -211.11. IR (ATR) $\tilde{\nu}_{max}$ (cm^{-1}): 2958, 2856, 1611 (C=O), 1578 (C=N), 1500, 1339, 710 (Sn–O); UV/Vis ($CHCl_3$): $\lambda_{abs/max}$, $\varepsilon_{max}*10^4$: 457 nm, 2.69 $M^{-1}cm^{-1}$. Anal. Calc. for $C_{26}H_{36}N_4O_4Sn$: C, 53.17; H, 6.18; N, 9.54; Found: C, 53.06; H, 6.49; N, 8.90.

[N-(4-diethylamino-2-oxidobenzylidene)-4-nitrobenzyhydrazidato] diphenyltin(IV) **6**

The procedure was similar to the synthesis of **1** as red solid (80%). M. p. 260 °C. ^{1}H NMR (400 MHz, $CDCl_3$, 298 K): δ 1.27 (t, 6H, *J* = 7.2 Hz, CH_3), 3.43 (q, 4H, *J* = 7.2 Hz, CH_2), 6.19 (dd, 1H, *J* = 4, 8 Hz, H-5), 6.26 (s, 1H, H-3), 6.98 (d, 1H, *J* = 8.8 Hz, H-6), 7.41 (m, 4H, H-*m*/H-*p*), 7.90 (s, 4H, $^{3}J(^{1}H,^{119}Sn)$ = 75 Hz, H-*o*), 8.26 (d, 2H, *J* = 8.8 Hz, H-10/14), 8.32 (d, 2H, *J* = 8.8 Hz, H-11/13), 8.47 (s, 1H, $^{3}J(^{1}H,^{119}Sn)$ = 56.4 Hz, H-7). ^{13}C NMR (100 MHZ, $CDCl_3$, 298 K): δ 13.03 (C-16,18), 44.91 (C-15,17), 104.68 (C-4), 101.06 (C-2), 107.26 (C-6), 128.26 (C-10,14), 123.57 (C-11,13), 128.96 (C-*m*, $^{3}J(^{119}Sn,^{13}C)$ = 84.30 Hz), 136.37 (C-*o*, $^{2}J(^{119}Sn,^{13}C)$ = 54.0 Hz), 130.51 (C-*p*, $^{4}J(^{119}Sn-^{13}C)$ = 19 Hz), 136.89 (C-5), 140.26 (C-*i*, $^{1}J(^{119}Sn,^{13}C)$ = 1079 Hz), 149.02 (C-12), 139.88 (C-9), 154.59 (C-3), 161.00 (C-7, $^{2}J(^{119}Sn,^{13}C)$ = 25.40 Hz), 164.58 (C-1), 169.70 (C-8); $^{1}H/^{13}C$ HETCOR correlation [δ_H/δ_C]: 1.27/13.03 (H-16,18/C-16,18), 3.46/44.91 (H-15,17/C-15,17), 6.2/104.68 (H-4/C-4), 6.28/101.06 (H-2/C-2), 7.0/136.89 (H-5/C-5), 7.44/128.96 (H-*m*/C-*m*), 7.48/130.51 (H-*p*/C-*p*), 7.92/136.37 (H-*o*/C-*o*), 8.28/128.26 (H-10,14/C-10,14), 8.35/123.57 (H-11,13/C-11,13), 8.50/161.0 (H-7/C-7); COSY correlation [δ_H/δ_H]: 1.27/3.46 (H-16,18/H-15,17), 6.21/7.00 (H-4/H-5), 7.44/7.92 (H-*m*/H-*o*), 8.28/8.35 (H-10,14/H-11,13). ^{119}Sn NMR (128 MHz, $CDCl_3$, 298 K): δ -328. IR (ATR) $\tilde{\nu}_{max}$ (cm^{-1}): 2923, 2868, 1611 (C=O), 1576 (C=N),

1503, 1334, 733(Sn–O) cm^{-1}. $\lambda_{abs/max}$, $\varepsilon_{max}*10^4$: 454 nm, 6.30 $M^{-1}cm^{-1}$. Anal. Calc. for $C_{30}H_{28}N_4O_4Sn{\cdot}H_2O$: C, 55.84; H, 4.69; N, 8.68; Found: C, 55.47; H, 4.55; N, 8.54.

[N-(4-methoxy-2-oxidobenzylidene)-4-nitrobenzyhydrazidato] di-n-butyltin(IV) **7**

The procedure was similar to the synthesis of **1** as yellow solid (98 %). M. p. 106 °C. ^{1}H NMR (400 MHz, $CDCl_3$, 298 K): δ 0.87 (t, 6H, *J* = 7.6 Hz, H-δ), 1.36 (sx, 4H, *J* = 7.6 Hz, H-γ), 1.53 (m, 4H, H-α), 1.65 (m, 4H, H-β), 3.81 (s, 3H, H-15), 6.25 (d, 1H, *J* = 2.0 Hz, H-2), 6.35 (dd, 1H, *J* = 2.4, 8.8 Hz, H-4), 7.06 (d, 1H, *J* = 8.8 Hz, H-5), 8.20 (d, 2H, *J* = 9.2 Hz, H-10,14), 8.25 (d, 2H, *J* = 9.2 Hz, H-11,13), 8.64 (s, 1H, $^3J(^{119}Sn,^1H)$ = 43 Hz, H-7). ^{13}C NMR (100 MHz, $CDCl_3$, 298 K):) δ 13.71 (C-δ), 22.42 (C-α, $^1J(^{119/117}Sn,^{13}C)$ = 602/568 Hz), 26.56 (C-γ, $^3J(^{119}Sn,^{13}C)$ = 86.20 Hz), 26.94 (C-β, $^2J(^{119}Sn,^{13}C)$ = 34.7 Hz), 55.59 (C-15), 103.82 (C-2), 107.60 (C-4), 110.72 (C-6, $^3J(^{119}Sn,^{13}C)$ = 21.6 Hz), 123.45 (C-11,13), 128.41 (C-10,14), 135.99 (C-5), 139.93 (C-9), 149.15 (C-12), 162.13 (C-7, $^2J(^{119}Sn,^{13}C)$ = 19.50 Hz), 166.34 (C-1, $^2J(^{119/117}Sn,^{13}C)$ = 19.5/10.5 Hz), 166.68 (C-3), 170.05 (C-8, $^2J(^{119}Sn,^{13}C)$ = 31.4 Hz). HETCOR correlation [δ_H/δ_C]: 0.87/13.71 (H-δ/C-δ), 1.36/26.56 (H-γ/C-γ), 1.53/22.42 (H-α/C-α), 1.65/26.94 (H-β/C-β), 3.81/55.59 (H-15/C-15), 6.25/103.82 (H-2/C-2), 6.35/107.60 (H-4/C-4), 7.06/135.99 (H-5/C-5), 8.20/128.41 (H-10,14/C-10,14), 8.25/123.45 (H-11,13/C-11,13), 8.64/162.13 (H-7/C-7); COSY correlation [δ_H/δ_H]: 0.87/1.36 (H-δ/H-γ), 1.36/1.65 (H-γ/H-β), 1.53/1.65 (H-α/H-β), 6.35/7.06 (H-4/H-5), 8.20/8.25 (H-10,14/H-11,13). ^{119}Sn NMR (128 MHz, $CDCl_3$, 298 K): δ -187.04. IR (ATR) $\tilde{\nu}_{max}$ (cm^{-1}): 2916, 2854, 1604, 1592, 1526, 1339, 713; $\lambda_{abs/max}$, $\varepsilon_{max}*10^4$: 430 nm, 3.19 $M^{-1}cm^{-1}$. Anal. Calc. for $C_{23}H_{29}N_3O_5Sn$: C, 50.58; H, 5.35; N, 7.69. Found: C, 53.35; H, 6.67; N, 7.56.

[N-(4-methoxy-2-oxidobenzylidene)-4-nitrobenzyhydrazidato] diphenyltin(IV) **8**

The procedure was similar to the synthesis of **1** as yellow solid (81%). M. p. 224 °C. ^{1}H NMR (400 MHz, $CDCl_3$, 298 K): δ 3.91 (s, 4H, H-15,17), 6.41 (dd, 1H *J* = 2.4, 8.8 Hz, H-4), 6.59 (d, 1H, *J* = 2.0 Hz, H-2), 7.09 (d, 1H, *J* = 8.8 Hz, H-5), 7.48 (m, 4H, H-*p*), 7.46 (m, 4H, H-*m*), 7.90 (d, 4H, $^3J(^{119/117}Sn,^1H)$= 88/73.6 Hz, H-*o*), 8.29 (d, 2H, *J* = 8.8 Hz, H-

10,14), 8.36 (d, 2H, J = 8.8 Hz, H-11,13), 8.65 (s, 1H, $^{2}J(^{119}Sn,^{1}H)$ = 53.2 Hz, H-7). ^{13}C RMN (100 MHz, $CDCl_3$, 298 K): δ 55.52 (C-15), 104.34 (C-2), 108.16 (C-4), 110.78 (C-6), 123.54 (C-11,13), 128.50 (C-10,14), 128.08 (C-*m*, $^{3}J(^{119/117}Sn,^{13}C)$ = 86/84 Hz), 130.78 (C-*p*, $^{4}J(^{119}Sn,^{13}C)$ = 18 Hz), 136.21(C-*o*, $^{2}J(^{119}Sn,^{13}C)$ = 54 Hz), 136.27 (C-5), 139.07 (C-9), 139.54 (C-*i*, $^{1}J(^{119/117}Sn,^{13}C)$ = 987/943 Hz), 149.28 (C-12), 162.68 (C-7, $^{2}J(^{119}Sn,^{13}C)$ = 25 Hz), 167.0 (C-1), 165.89 (C-3), 170.29 (C-8, $^{2}J(^{119}Sn,^{13}C)$ = 31 Hz). HETCOR correlation [δ_H/δ_C]: 3.91/55.52 (H-15/C-15), 6.41/108.16 (H-4/C-4), 6.59/104.34 (H-2/C-2), 7.09/136.27 (H-5/C-5), 7.46/128.08 (H-*m*/C-*m*), 7.48/130.78 (H-*p*/C-*p*), 7.90/136.21 (H-*o*/C-*o*), 8.29/128.50 (H-10,14/C-10,14), 8.36/123.54 (H-11,13/C-11,13), 8.65/162.68 (H-7/C-7). COSY correlation [δ_H/δ_H]: 6.41/7.09(H-4/H-5), 7.46/7.90 (H-*m*/H-*o*), 8.29/8.36 (H-10,14/H-11,13). ^{119}Sn NMR (128 MHz, $CDCl_3$, 298 K): δ -328.23. IR (ATR) $\tilde{\nu}_{max}$ (cm^{-1}): 2852, 2837, 1606, 1584, 1527, 1216, 735. $\lambda_{abs/max}$, $\varepsilon_{max}*10^4$: 426 nm, 5.06 $M^{-1}cm^{-1}$. Anal. Calc. for $C_{27}H_{21}N_3O_5Sn$: C, 55.32; H, 3.61; N, 7.17; Found: C, 55.62; H, 3.75; N, 6.98.

2.3. X-ray crystallographic studies

The crystals of **1**, **2**, and **4** were covered with a layer of hydrocarbon oil that was selected and mounted with paratone-N oil on a cryo-loop, and immediately placed in the low-temperature nitrogen stream at 100(2) K. The data for **1**, **2**, and **4** were recorded on a Bruker SMART APEX CCD area detector system equipped with an Oxford Cryosystems 700 Series Cryostream cooler, a graphite monochromator, and a Mo Kα fine-focus sealed tube (λ = 0.71073 Å). The crystals data of **5** and **8** were recorded on an Enraf Nonius Kappa-CCD (λ MoKa=0.71073 Å, graphite monochromator, T = 293 K-CCD rotating images scan mode). The crystal was mounted on a Lindeman tube. The structures were solved by direct methods using SHELXS-97[18] and refined against F^2 on all data by full-matrix least-squares with SHELXL-97.[19] All of the software manipulations were done under the WIN-GX environment program set.[20] All heavier atoms were found by Fourier map difference and refined anisotropically. Some hydrogen atoms were found by Fourier map differences and refined isotropically. The remaining hydrogen atoms were geometrically modelled and are not refined. Crystallographic data for the structures reported in this paper have been deposited in the Cambridge Crystallographic Data Centre:

CCDC 1059889 for **1**, CCDC 1059890 for **2**, CCDC 1059888 for **4**, CCDC 1059373 for **5**, and CCDC 1059374 for **8**.

2.4. Photophysical characterization

For the photophysical characterization, spectroscopic grade CH_2Cl_2 from Aldrich was freshly distilled and the solutions were studied as prepared, in order to avoid any solvolysis or photodegradation effect.[21] UV-Vis absorption spectra were measured on a Shimadzu 2401PC spectrophotometer. The emission and excitation spectra have been recorded with a Perkin-Elmer LS 50B spectrofluorimeter. Excitation spectra were obtained by fixing as the emission wavelength the fluorescence maxima. Fluorescence quantum yields in solution (ϕ) were determined according to the procedure reported in literature[22] and using quinine sulphate in H_2SO_4 0.1 M (ϕ = 0.54 at 310 nm) as the standard. Measurements were carried out by controlling the temperature at 25.0±0.5 °C with a water circulating bath. Three solutions with absorbance at the excitation wavelength lower than 0.1 were analysed for each sample and the quantum yield was averaged. Lifetimes were obtained by TCSPC (Time-correlated single photon counting) with a Tempro Horiba equipment with a 455 nm nanoLED. A 0.01% suspension of Ludox AS40 (Aldrich) in ultrapure water was used for the prompt signal. Calibration of the equipment was realized with a POPOP [1,4-Bis(4-methyl-5-fenil-2-oxazolyl)benzene] methanol solution (optical density <0.1 and lifetime of 0.93ns).[23] Data were fit in the software DAS6 available in the equipment.

2.5. Cell image

B16F10 murine melanoma cells were seeded in 12 wells plates on poly-lysine (Sigma-Aldrich, St. Louis, MO) coated sterile coverslips at a density of $1x10^5$ cells/well in 1 mL of DMEM/F12 media (Invitrogen Life Technologies, Carlsbad, CA) supplemented with 10% fetal bovine serum (Gibco Life Technologies, USA) and maintained at 37 °C in a controlled humid atmosphere of 5% CO_2 and 95% air. Twenty four hours later the medium was renewed and cells were exposed to the compounds at a concentrations of 0.01 μg mL^{-1}, 1 μg mL^{-1}, and 10 μg mL^{-1} (0.065, 0.65, and 6.5 ppm, respectively) for two hours. Untreated cells or treated with DMSO were used as controls. Supernatants were removed and

coverslips were washed once with 1 mL of PBS, mounted on microscope slips using Vectashield (Vector Laboratories, Inc. Burlingame, CA) and imaged using confocal laser microscopy (Leica TCS SP5 Confocal System). Samples were excited at 458 nm and the fluorescence emission was measured at 478-612 nm for all compounds except compound **3**, which emission was measured at 475-550 nm.

2.6. Cytotoxicity assays in cells

B16F10 murine melanoma cells were seeded in 96 wells plates at a density of $1x10^4$ cells per well in 100 μL of media and incubated for 24 hours at 37 °C. Medium was exchanged and compounds were added at concentrations ranging from 0.01 μg mL^{-1} to 10 μg mL^{-1}. Untreated cells or treated with dimethyl sulfoxide (DMSO, Sigma-Aldrich Co, St. Louis, MO) were used as controls. Twenty four hours later 10 μL of alamarBlue (Biosource Invitrogen Life Technologies, Carlsbad, CA) were added to each well. Viability of the cultures was measured as reagent colour change by spectrophotometry on an ELISA Microplate Reader (Biotek Multiskan ELX800, BioTek Instruments, Inc, Winooski, VT) at dual wavelength of 570 and 600 nm according to manufacturer´s instructions.

3. Results and discussion

3.1. Synthetic procedures

The reaction in one-pot of 2-hydroxynaphtaldehyde, benzhydrazine and the corresponding diorganotin oxide provided the pentacoordinated organotin derivatives in good yields (80-98%) as red, orange or yellow solids (**1-8**), while **3** was brown oil. All organotin compounds were air-stable and soluble in common organic solvents. Compound **4** was poorly soluble with the exception of dimethyl sulfoxide (*vide infra*).

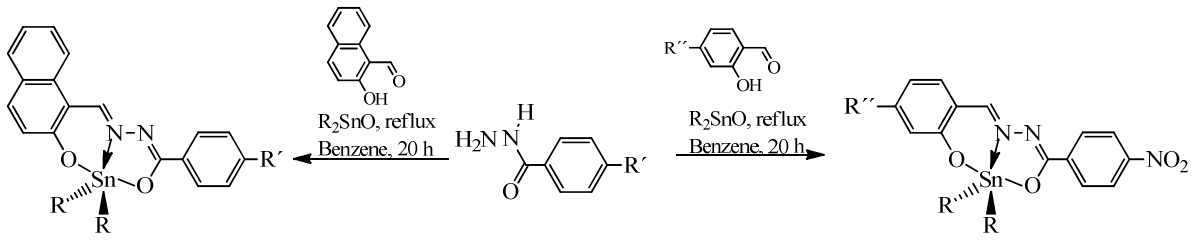

1: R = *n*Bu, R′= NO_2
2: R = Ph, R′= NO_2
3: R = *n*Bu, R′= H
4: R = Ph, R′= H

5: R = *n*Bu, R′′ = Et_2N
6: R = Ph, R′′ = Et_2N
7: R = *n*Bu, R′′ = MeO
8: R = Ph, R′′ = MeO

Scheme 1 Synthesis of organotin compounds **1-8**.

3.2. Spectroscopic characterization.

The ^{119}Sn NMR spectra ($CDCl_3$) of dibutyltin derivatives (**1**, **3**, **5** and **7**) show a single resonance within the range of -187 and -211 ppm (Table 1), while the diphenyl tin complexes (**2**, **6**, and **8**) are around -327 ppm. In both series there are characteristics of pentacoordinated tin atoms in noncoordinating solvent, where the tin atoms reside in trigonal bipyramidal molecular geometry.[24,25,26] However, compound **4** shows a δ ^{119}Sn at -407 ppm in deuterated dimethylsulfoxide (DMSO-d_6) having a characteristic of a hexacoordinated tin atom.[27] This effect must be explained on the basis of DMSO coordinated to tin atoms allowing intermolecular interactions. In the ^{13}C NMR spectra for all of the organotin compounds, the signals of the imine carbon, C7 or C11 appear in the range from 156 to 162 ppm, which are deshielded with respect to free ligands, due to the N→Sn coordination bond. Indeed, the ^{13}C δ of imine group showed $^{3}J(^{119}Sn,^{13}C)$ around 22 Hz. Additionally, the C-Sn-C bond angles 133.8°, 134.2°, 135° and 134.9° for **1**, **3**, **5** and **7** respectively, were calculated by using the $^{1}J(^{119}Sn,^{13}C)$ and the Holeček equations [28] values, suggesting that the tin atoms have a slightly distorted trigonal bipyramid geometry in $CDCl_3$. Also, C-Sn-C bond angles for diphenyltin derivatives (**6**: 144.3°, **8**: 116.3°) were calculated showing the same geometrical distortion.[29] The δ ^{1}H of imine protons (H-11) for **1-8** are observed in the range of 8.47-9.71 ppm and the $^{3}J(^{1}H\text{-}N\text{-}^{119}Sn)$ of 44 and 62 Hz, confirming the presence of N→Sn coordination bonds (Figure 1), which is agree with previous reports.[30] The IR spectra show four intense bands for C=N, C-O, Sn-C and Sn-O

at about 1684, 1444, 1430 and 710 cm^{-1} respectively.[31] The elemental analysis confirmed the proposed structures of compounds **1**-**8**.

3.3. X-ray diffraction analyses for 1, 2, 4, 5 and 8.

The crystal structures of compounds **1**, **2**, **4**, **5**, and **8** were determined by X-ray diffraction (Table 2) and are depicted in figures 1 and 2. Selected bond lengths and angles are listed in Table 3. In all cases, the central tin atoms are five-coordinated with distorted trigonal bipyramidal molecular geometry (O-Sn-O range angle 154.96-157.54°, C-Sn-C from 120 to 132°), which mainly results from the strained five-membered Sn-N-N-C-O chelate ring and the ligand taken on a nearly rigid planar structure.

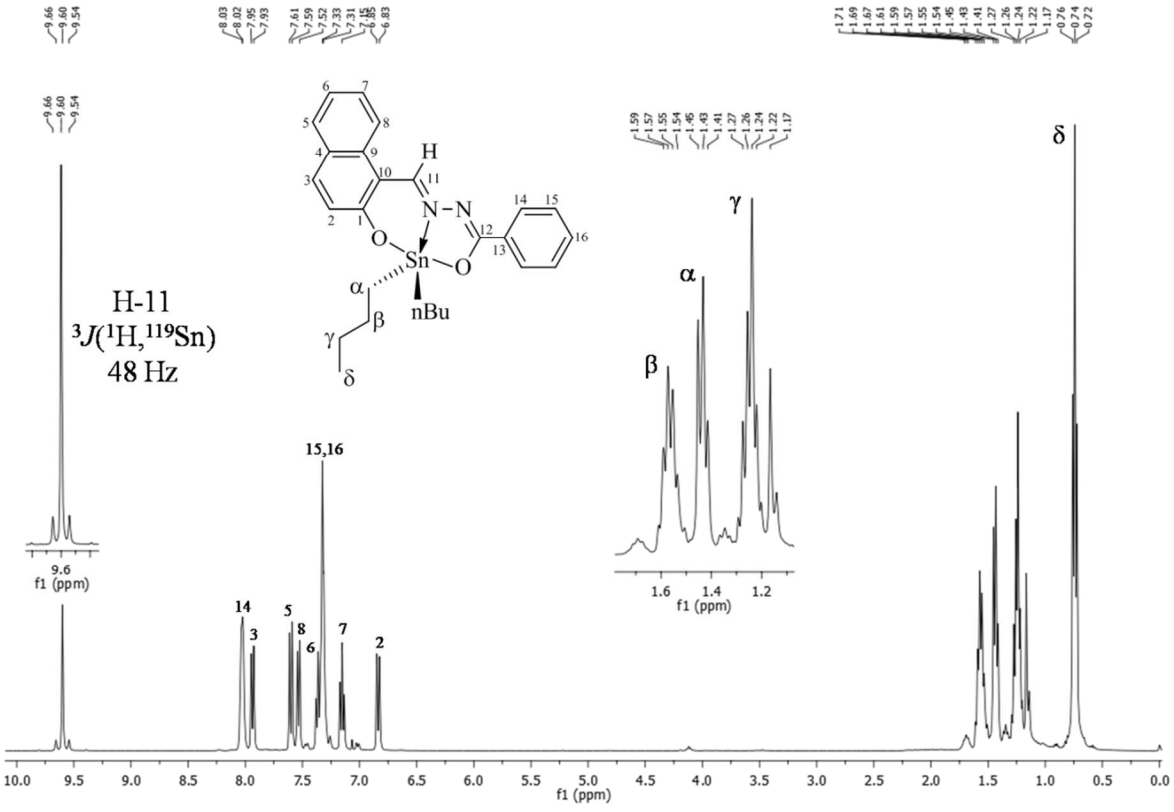

Fig. 1. ^1H NMR ($CDCl_3$) spectrum of compound **3.**

However, the dihedral angle between the outer benzene ring and the naphthyledene or salicylidene plane is 8.98° for **1**, 19.8° for **2**, 18.33° for **4**, 8.8° for **5**, and 9.1° for **8**, indicating no coplanar framework. The N-Sn distances (**1**: 2.157(2), **2**: 2.143(3), **4**: 2.1478(15), **5**: 2.136(4), **8**: 2.150(3) Å) are shorter than similar benzylidenebenzyhydrazidato pentacoordinated tin complexes (2.1720(17) Å) reported by Lo and Chow.[32] The bond lengths of Sn-O1 and Sn-O2 are ranging from 2.072(2) to 2.102(2) Å and from 2.1203(13) to 2.151(4) Å respectively, excluding quinone structures. The five crystal structures show parallel-displaced π-π interactions in the range from 3.258 Å to 3.627 Å (Figures 2 and 3). In the asymmetric unit of **1** there are two independent molecules, which form a planar central four-membered Sn_2O_2 core with Sn···O distances of 3.818 and 4.231 Å (See supporting information). It is comparable with organotin Schiff bases already reported.[33]

Table 1 Selected ^{1}H ($^{n}J^{1}H$-^{119}Sn), ^{13}C [$^{n}J^{13}C$-^{119}Sn], and ^{119}Sn (ppm) and stretching vibrations of the C=N bonds (cm^{-1}).

Comp.	^{1}H	^{13}C				^{119}Sn	IR
	H-11/H-7	C-11/C-7	C-α/C_i	C-1	C-12/C8		(C=N)
1	9.68 (48)	158.2 [20]	22.3 [591/565]	170.0	166.1	-189.8	1597
2	9.71 (62)	158.4	138.5	170.2	165.8	-327.2	1596
3	9.60 (48)	156.7 [20]	22.0 [595/576]	169.4 [34]	168.5 [10]	-189.9	1598
4[a]	9.59 (52)	157.2	139.1	169.6	168.2	-406.7[a]	1599
5	8.50 (46)	160.9 [22]	22.14 [603/577]	165.02	169.2 [31]	-211.1	1578
6	8.47 (56)	161.0 [25]	140.2 [1079]	164.5	169.7	-328.0	1576
7	8.65 (43)	162.1 [19.5]	22.4 [602/568]	166.5	169.8 [31.4]	-187.0	1592
8	8.62 (53)	162.6 [25]	138.9 [987/943]	167.0	170.2 [31]	-328.2	1584

[a] DMSO-d_6

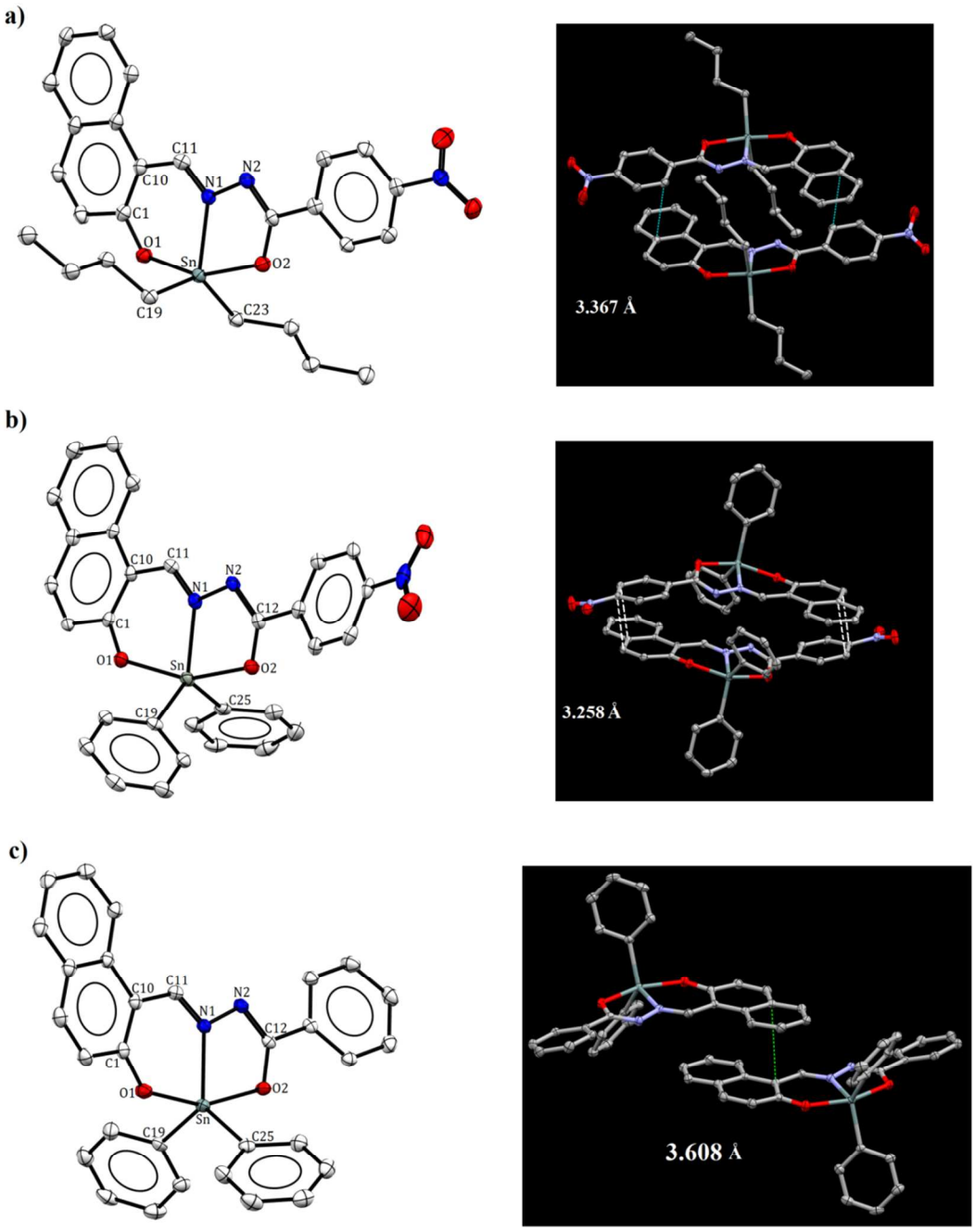

Fig. 2 Molecular structures of a) **1**, b) **2**, and c) **4** with labeling scheme. Stacking interactions are shown by dashed lines. The anisotropic displacement parameters are depicted at the 50% probability level. All hydrogen atoms are omitted for clarity.

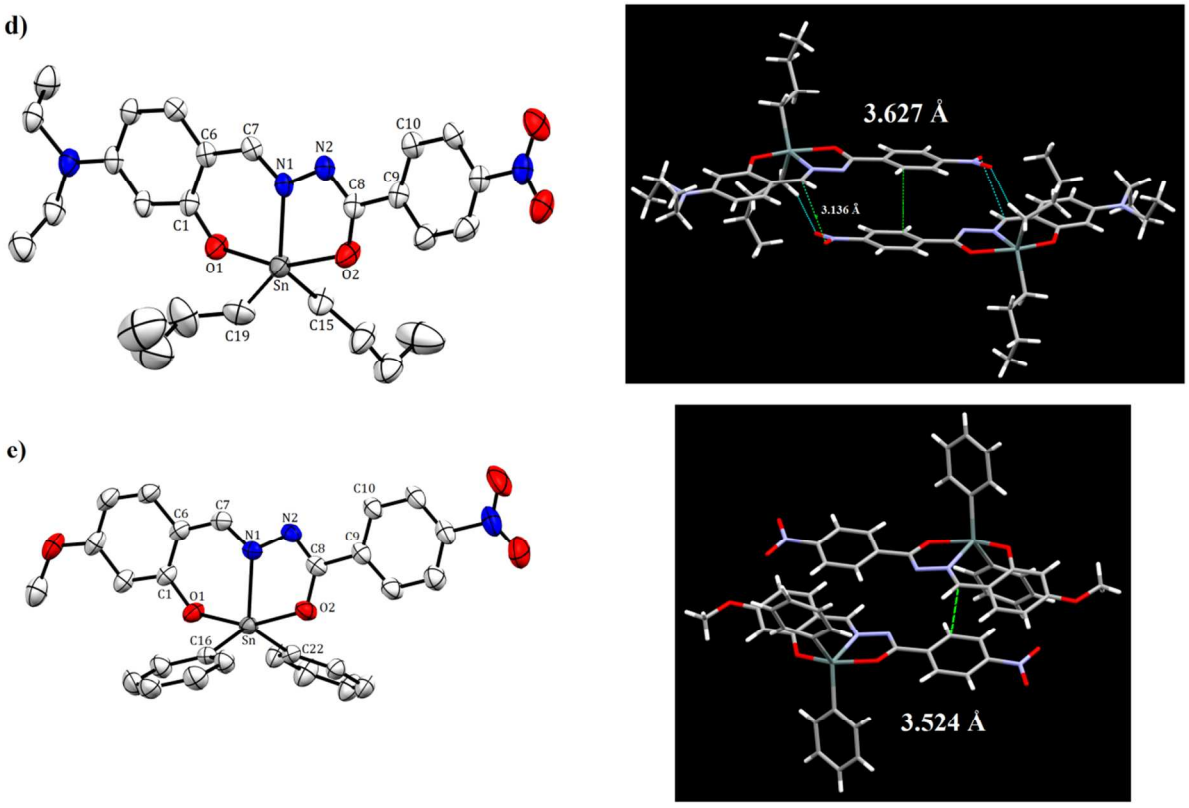

Fig. 3 Molecular structures of d) **5** and e) **8** with labeling scheme. Stacking interactions are shown by dashed lines. The anisotropic displacement parameters are depicted at the 50% probability level. All hydrogen atoms are omitted for clarity.

Table 2 Crystal data for compounds **1**, **2**, **4**, **5**, and **8**.

	1	**2**	**4**	**5**	**8**
Empirical formula	$C_{26}H_{29}N_3O_4Sn$	$C_{30}H_{21}N_3O_4Sn$	$C_{30}H_{22}N_2O_2Sn$	$C_{26}H_{36}N_4O_4Sn$	$C_{27}H_{21}N_3O_5Sn$
Formula weight	566.21	606.19	561.19	587.28	586.16
Temperature, K	100(2)	100(2)	100(2)	293(2)	293(2)
Wavelength	0.71073	0.71073	0.71073	0.71073	0.71073
Cryst size, mm^3	0.15x0.07x0.05	0.15x0.05x0.04	0.12x0.11x0.10	0.325x0.075x0.025	0.23x0.13x0.06
Crystal system	Triclinic	Triclinic	Monoclinic	Monoclinic	Triclinic
Space group	*P*-1	*P*-1	*P*21/*c*	C 2/*c*	*P*-1
a, Å	11.1871(13)	9.9567(18)	9.8450(12)	19.7987(4)	8.6061(2)
b, Å	15.2135(18)	10.633(2)	8.6454(10)	10.3272(3)	11.9693(2)
c, Å	17.015(2)	12.581(2)	28.744(3)	27.5213(4)	12.7463(2)
α	109.4080(10) °	111.606(2) °	90 °	90.00	105.8720(10)
β	98.1620(10) °	93.531(2) °	93.0780(10) °	95.5150(10)	91.9980(10)
γ	110.7710(10)°	93.129(2) °	90 °	90.00	95.7250(10)
V,$Å^3$	2440.5(5)	1231.8(4)	2443.0(5)	5601.1(2)	1253.97(4)
Z	4	2	4	8	2
$\rho_{calc,Mg.cm-3}$	1.541	1.634	1.526	1.393	1.552
μ, mm^{-1}	1.084	1.081	1.076		
2θ range for data collection	1.33 – 28.32 °	1.75 – 28.37 °	1.42 – 28.3 °		
Index ranges	$-14 \le h \le 14$, $-20 \le k \le 20$, $-22 \le l \le 22$	$-13 \le h \le 13$, $-14 \le k \le 14$, $-16 \le l \le 16$	$-13 \le h \le 13$, $-11 \le k \le 11$, $-38 \le l \le 38$	$-23 \le h \le 25$, $-13 \le k \le 10$, $-35 \le l \le 35$	$-10 \le h \le 11$, $-15 \le k \le 15$, $-16 \le l \le 15$
No. reflns collected	24265	12280	23387	24781	25185
No. indep reflns	11974	6068	6086	6389	5695
[R_{int}]	0.0307	0.0408	0.0266		
Goodness of fit	1.039	1.013	1.065	1.019	1.225
*R*1, w*R*2 (I>2σ(I))	0.0407	0.0457	0.0287	0.1511	0.0469
	0.0976	0.1025	0.0730	0.1315	0.0365
*R*1, w*R*2 (all data)	0.0520	0.0566	0.0310	0.0892	0.1035
	0.1046	0.1085	0.0748	0.0550	0.0972
$\Delta\rho_{min}$ (e $Å^{-3}$)	- 0.767	- 0.687	- 0.656	-1.018	-1.056
$\Delta\rho_{max}$ (e $Å^{-3}$)	2.151	1.540	1.552	1.702	0.467

Table 3 Selected bond distances (Å) and angles (°) for **1**, **2**, **4**, **5**, and **8**.

	1	**2**	**4**		**5**	**8**
Sn-O(1)	2.102(2)	2.072(2)	2.0773(13)	Sn-O (1)	2.075 (4)	2.074 (3)
Sn-O(2)	2.139(2)	2.126(2)	2.1203(13)	Sn-O (2)	2.151 (4)	2.127 (2)
Sn-N(1)	2.157(2)	2.143(3)	2.1478(15)	Sn-N (1)	2.136 (4)	2.150 (3)
Sn-C(19)	2.131(3)	2.113(3)	2.1101(19)	Sn-C (15)	2.104 (8)	2.118 (3)
Sn-C(23)	2.129(3)			Sn-C (19)	2.129 (6)	
Sn-C(25)		2.130(4)	2.1164(18)	Sn-C (21)		2.119 (3)
C(1)-O(1)	1.321(3)	1.321(4)	1.305(2)	C(1)-O(1)	1.314 (5)	1.322 (4)
C(10)-C(11)	1.430(4)	1.421(5)	1.426(3)	C(8)-O(2)	1.300 (6)	1.300 (4)
C(11)-N(1)	1.308(4)	1.307(4)	1.303(2)	C(1)-C(7)	1.419 (6)	1.415 (5)
N(1)-N(2)	1.409(3)	1.407(4)	1.403(2)	N(1)-N(2)	1.404 (5)	1.399 (3)
N(2)-C(12)	1.308(4)	1.305(4)	1.309(2)	N(2)-C(8)	1.291 (5)	1.304 (5)
C(12)-O(2)	1.303(3)	1.296(4)	1.305(2)	C(7)- N(1)	1.303 (5)	1.305 (5)
C(19)-Sn-C(23)	131.03(11)			C(19)-Sn-C(15)	123.4 (3)	
C(19)-Sn-C(25)		122.50(13)	120.13(7)	C(21)-Sn-C(15)		132.76 (10)
O(1)-Sn-O(2)	154.96(8)	155.25(10)	157.04(5)	O(1)-Sn-O(2)	157.06 (15)	157.54 (10)
N(1)-Sn-C(19)	106.77(10)	123.70(12)	123.30(6)	N(1)-Sn-C(19)	121.51 (19)	
N(1)-Sn-C(23)	122.19(10)			N(1)-Sn-C(21)		112.73 (10)
N(1)-Sn-C(25)		113.49(12)	116.30(6)	N(1)-Sn-C(15)	114.7 (2)	114.22 (9)
O(1)-Sn-C(19)	96.13(9)	94.74(12)	96.80(6)	N(1)-Sn-O(2)	73.07 (13)	73.43 (10)
O(1)-Sn-C(23)	91.69(9)			N(1)-Sn-O(1)	84.39 (13)	84.25 (10)
O(1)-Sn-C(25)		98.08(12)	95.43(6)	O(2)-Sn-C(15)	94.2 (3)	93.26 (10)
O(2)-Sn-C(19)	97.45(10)	92.57(11)	94.06(6)	O(2)-Sn-C(19)	95.44 (18)	
O(2)-Sn-C(23)	131.03(11)			O(2)-Sn-C(21)		95.06 (10)
O(2)-Sn-C(25)		97.82(12)	96.50(6)	O(1)-Sn-C(15)	99.1 (3)	93.68 (11)

3.4. UV-vis absorption and photoluminescence

Table 4 collects the photophysical properties of the tin complexes in CH_2Cl_2. Figure 4 shows the electronic absorption spectra of naphthalene and phenylene (inserted) salycilydine tin complexes in CH_2Cl_2. In general all of the compounds present a main peak in the visible, with maximum wavelength ranging between 426 and 460 nm, which can be ascribed to the HOMO-LUMO electronic transition. The position of the maximum depends on the electronic delocalization through the molecules that is chemically modulated by 1) varying the electron donor (naphtyl for **1-4** or p-substituted phenyl for **5-8**) and by the electron withdrawing groups (nitro substituent) or hydrogen and by 2) changing the R ligand, n-butyl or phenyl. We found that the different electron donor or withdrawing groups clearly affect the push-pull character of the conjugated diimine segment. However, the overall conjugation depends also on the position of the tin atom; *in* or *out* of the plane,

which in turns depends also on the nature of the R ligands. As a general remark, we can observe that the band assigned to the naphtyl tin complexes **1-4,** exhibits excitonic features with a vibronic replica, that is 25 nm red shifted with respect to the (0,0) electronic transition. This behavior is not observed in **5-8,** where a broad band appears, suggesting a better molecular order for the naphtyl complexes. Additionally an UV band at 330-350 nm can be observed, which assignment is later discussed. The emission properties of **3** and **4** present different spectral features with respect to the rest of the complexes: i) both exhibit excitonic fluorescence spectra with maximum at around 480 nm and the vibronic replica centered at around 510 nm, ii) the fluorescence quantum yields (ϕ) are large, of 36 and 56%, contra 0.02-0.4% for the rest of the compounds. As expected iii) their fluorescence lifetime τ is shorter (around 3.8 ns) than the other complexes that present τ of $10^{-10}/10^{-11}$ s, such as similar Tin and Boron organocomplexes reported in literature.[34,35] iv) The fluorescence spectrum for both **3** and **4** does not change with the excitation wavelength in shape or bands position, as shown in Figure 5 for **4**. Moreover, v) the excitation spectrum recorded by fixing the more intense peak or the shoulder is the same (Figure 6). These two behaviors indicate that there is only one emitting species related to the same electronic transition. As vi) the excitation spectrum matches well with the absorption one (Figure 6), we can conclude that the bands observed in the UV region of the absorption spectra for **3** and **4** are associated to electronic transitions from underlying molecular orbitals to LUMO, rather than to the π-π^* intraligand absorptions that would have corresponded to the emission of the naphtyl or phenylimine segment. On the contrary, the fluorescence spectra of complexes **1**, **2** and **5-8** change in both shape and bands position with the excitation wavelength. Figure 7 shows the fluorescence spectra of **5** at different excitation wavelengths as an example, where it can be observed that the fluorescence bands become more broader and shift from the UV (382 nm) up to orange region (469 nm) by changing the excitation wavelength from 320 nm to 420 nm. The corresponding excitation spectrum also changes and in Figure 8, two representative spectra for **5** are reported. Deviations from the Kasha's rule are observed for fluorophores either that exist in two ionization states or that emit in the S_2 state.[36] Most of the transition metal complexes give rise to charge-transfer (MLCT) states, from metal-to-ligand that become essentially localized on one ligand extremely rapidly.[37] Glazer *et al.* reported, however, dual emission from

phenanthroline complexes of Ruthenium and he ascribed this unusual behavior to the fact that the MLCT is not localized.[38] In previous studies, we found that organoboron complexes derived from salicylidenebenzohydrazide presented very low quantum yields (<0.4%) and the fluorescence spectra did not change with the excitation wavelength.[35] In contrast, organotin complexes derived from 2-hydroxynaphthaldeyde showed one order larger quantum yields and the fluorescence spectra presented two emission bands by exciting in the UV. In ref. 35, the high energy fluorescence was assigned to the naphtoyl group emission, as the corresponding excitation spectrum matched well with the UV band in the absorption spectrum. The red shifted emission was attributed to MLCT emission, as its excitation spectrum corresponded to the complete absorption spectrum. For those complexes, however, the two fluorescence bands did not shift by changing the excitation wavelength, they just change their relative intensity.[35]

Table 4 Optical properties of compounds **1-8** in CH_2Cl_2.

Dye	λ_{abs} [nm]	ε [10^4 M^{-1} cm^{-1}]	λ_{em}[nm][a]	Φ [%]	τ[ns]
1	354, 453	3.78	411 (350)	0.16	$7.0x10^{-2}$
			484 (420)	0.12	
2	348, 460	3.56	413 (350)	0.19	$9.78x10^{-2}$
			529 (440)	0.24	
3	333, 346	2.33	4.82 (420)	56.0	3.89
	440				
4	334, 348	1.74	479 (420)	36.2	3.78
	435, 459				
5	364, 459	6.02	422 (350)	0.44	2.60×10^{-2}
6	362, 456	4.47	421 (350)	2.50	$2.74\ 10^{-2}$
			470 (420)	0.06	
7	328, 430	3.47	417 (350)	0.24	$1.43\ 10^{-1}$
			485 (420)	0.02	
8	330, 426	3.75	377 (310)	1.50	$1.98\ 10^{-1}$
			537 (410)	0.29	

[a] in parenthesis, the excitation wavelength

According to the study of EC Glazer, we assume that the MLCT state for **3** and **4** is localized on the entire molecule as occurs in most of the small organic molecules, where the excited states involve orbitals that are extending over the entire molecule. The other complexes having the nitro substituent in *para* position of the salicylidene moiety (contrary to **3** and **4** that have H), exhibit an emission that changes with the excitation wavelength, likely because the MLCT state is localized on different ligands depending on the excitation energy. A deeper photophysical and theoretical study is currently in progress in order to better understand this interesting behavior. However, for the purpose of the present work that is focused on the bioimaging properties of the tin complexes, the most promising materials are **3** and **4** because of their higher quantum yield.

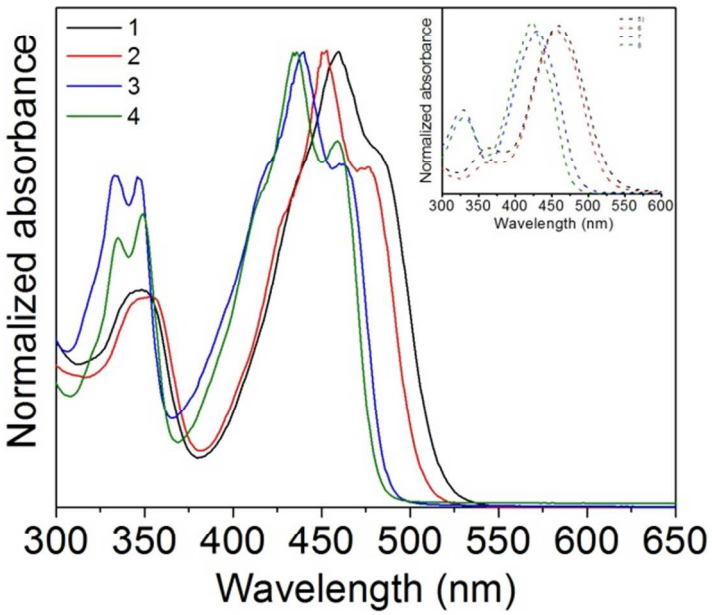

Fig. 4 UV-Vis spectra of compounds **1-8** in CH_2Cl_2

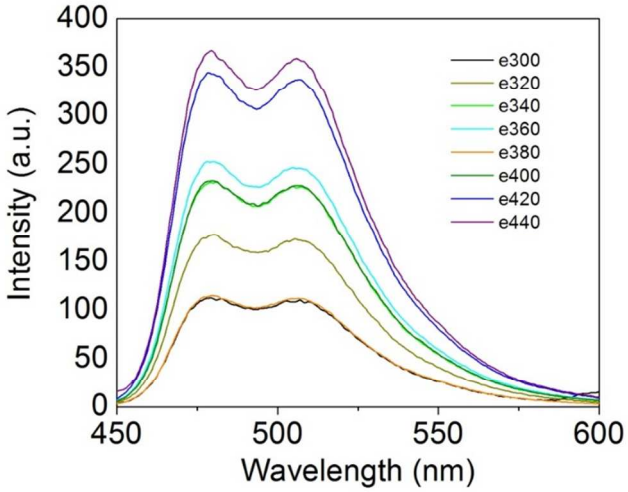

Fig. 5 Fluorescence spectra of **4** in CH_2Cl_2 at different excitation wavelengths.

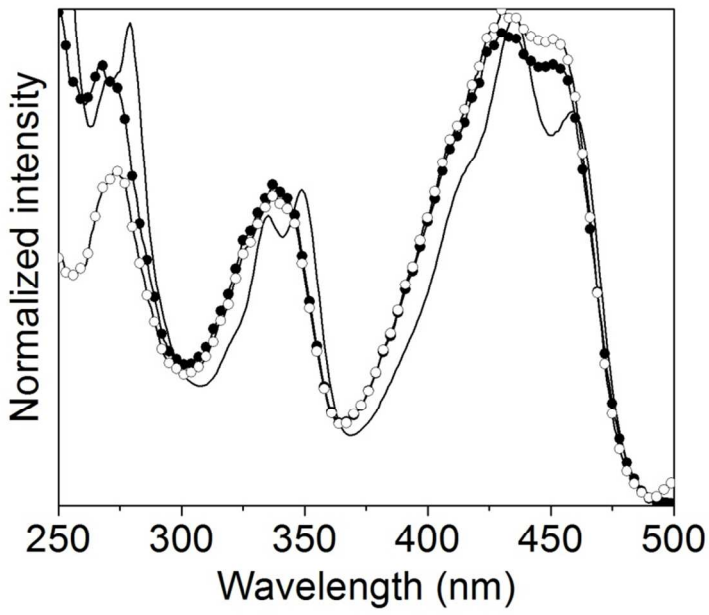

Fig. 6 Normalized excitation spectra of **4** in CH_2Cl_2 by fixing the emission peak at 479 (full circles) and 507 nm (empty circles). Normalized UV-Vis spectrum (solid line) is included.

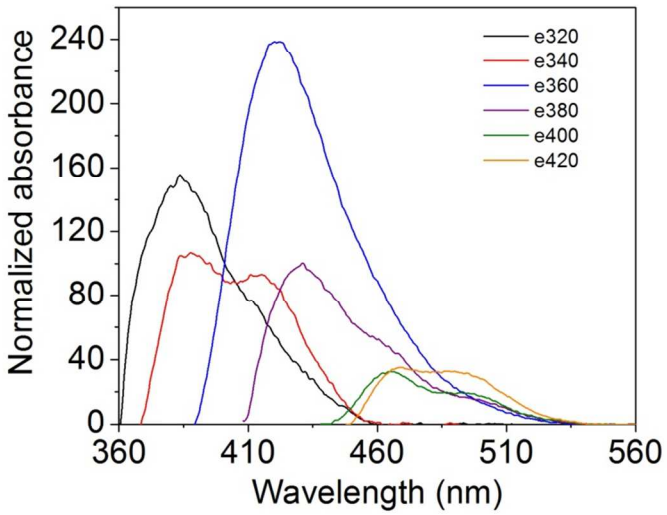

Fig. 7 Fluorescence spectra of **5** in CH_2Cl_2 at different excitation wavelengths.

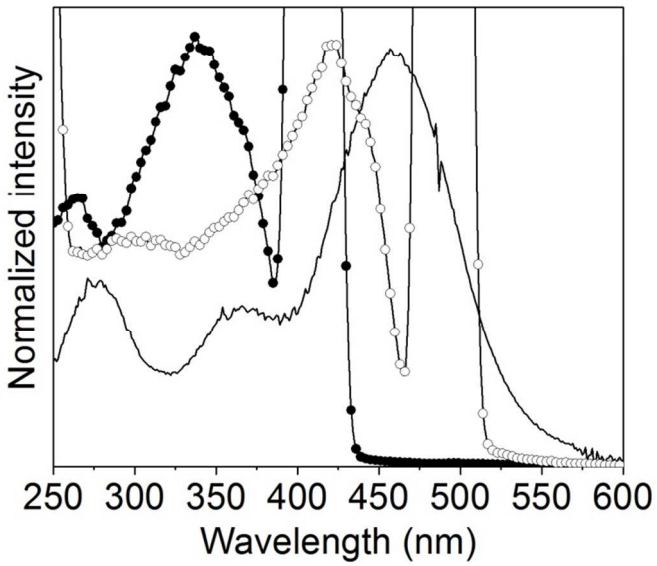

Fig. 8 Normalized excitation spectra of **5** in CH_2Cl_2 by fixing the emission peak at 422 (full circles) and 494 nm (empty circles). Normalized UV-Vis spectrum (solid line) is included

3.5. Cytotoxicity assay

Organotin compounds were used on tissue culture in order to assess their cytotoxic effects. B16F10 Cells were treated with five different concentrations of the compounds (10, 5, 2.5, and 1 μg mL^{-1}) for 24 hours and then viability was determined. As DMSO was the dissolvent used for the compounds, its toxicity was analyzed as well (Figure 9). The viability of the cells was greatly affected at the higher tested concentrations (10 μg mL^{-1}), being compounds **1**, **3**, **4**, and **7** the more toxic, while compounds **2**, **5**, and **8** produced a slightly lower toxicity, being compound **6** the less toxic overall. It is worth mentioning that DMSO solutions of all of the compounds retained their toxicity for several months, with exception of compound **3**. With freshly synthesized compound, we observed a toxicity of approximately 96% (Figure 9), but when we repeated the experiment 3 months later, it was down to approximately 30% (data not shown).

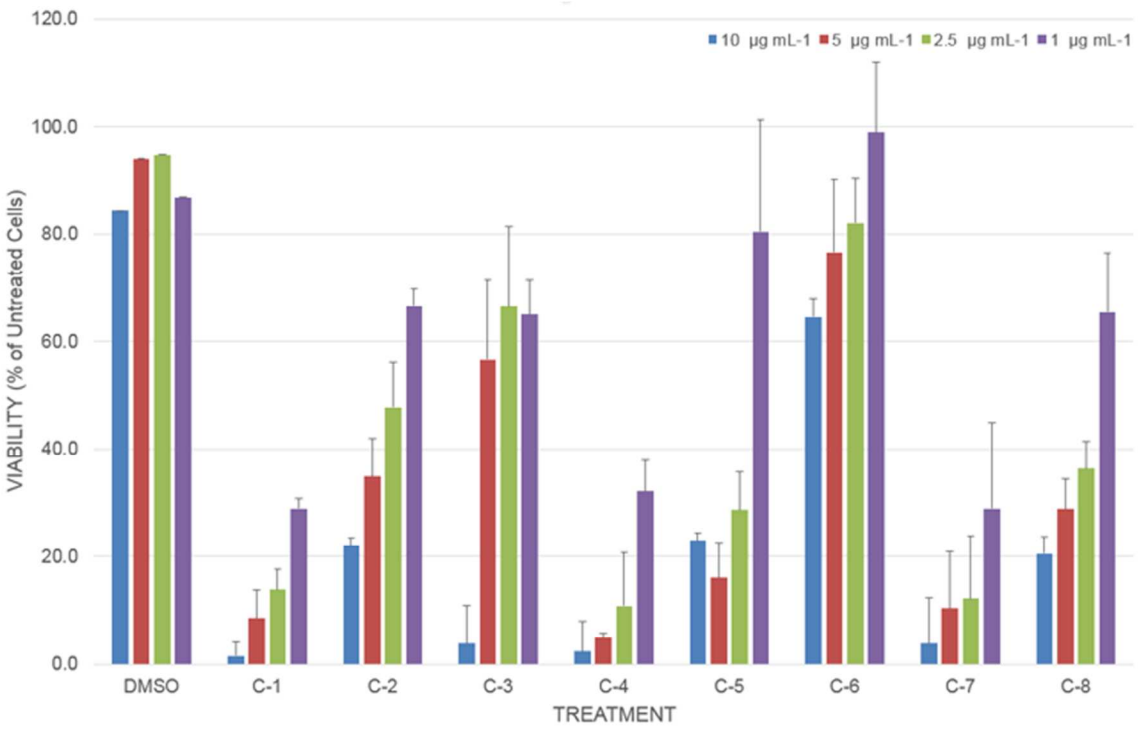

Fig. 9 Cytotoxic effect of organotin compounds. Melanoma cells B16F10 were treated with 10 μg mL^{-1} (blue bars), μg mL^{-1} (red bars), 2.5 μg/ml (green bars), or 1 μg mL^{-1} (purple bars) for 24 hours. As controls, cells treated with DMSO and untreated cells were used. (Data represents media +/- SD of three independent experiments).

More interesting, its staining capacity remained intact (data not shown), suggesting a partial degradation of the compound to still fluorescent metabolites and not to the original reagents shown in scheme 1. When lower concentrations of compounds were used, a dose-dependent response tendency was observed for all of the compounds. At 1 μg mL^{-1} only compounds **1**, **4**, and **7** remained very toxic. As compounds **3**, **4**, and **5** produced the best staining in cells, and compounds **3** and **5** were able to stain cells even at low concentrations, we determined their cytotoxic effects at those concentrations. Figure 10 shows that results for compounds, **4** and **5**, at 0.1 mg mL^{-1} are practically innocuous to cells, while compound **3** is still moderately toxic.

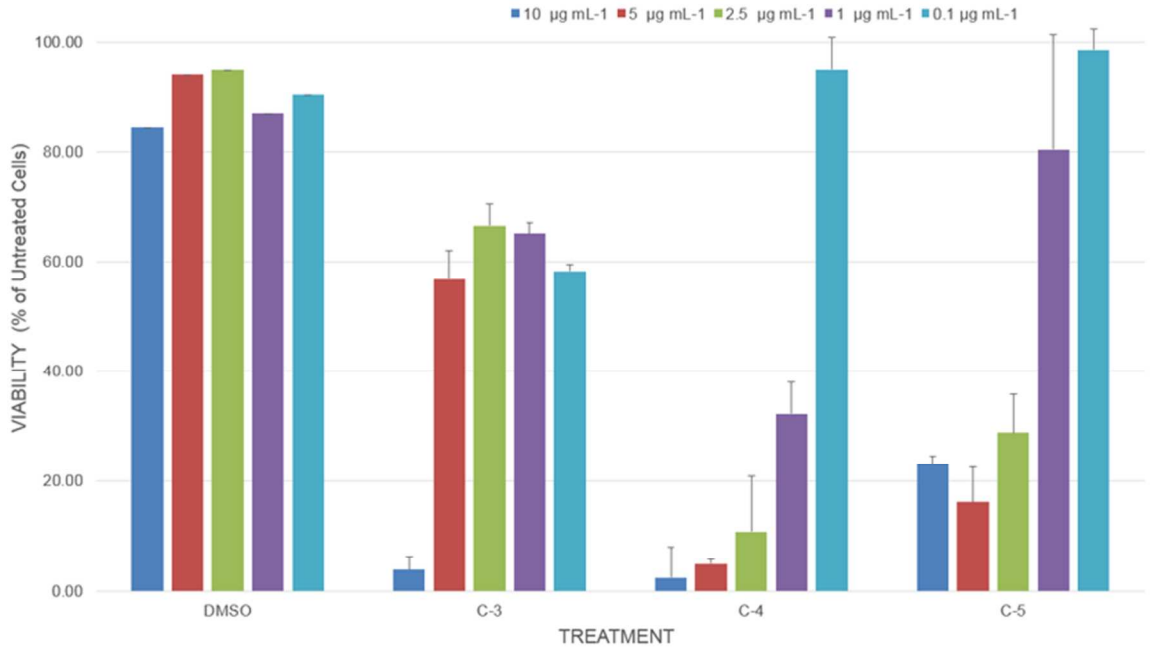

Fig. 10 Cytotoxic effects of organotin compounds **3**, **4**, and **5**. Melanoma cells B16F10 were treated with 10 μg mL^{-1} (blue bars), 5 μg mL^{-1} (red bars), 2.5 μg mL^{-1} (green bars), 1 μg mL^{-1} (purple bars), or 0.1 μg mL^{-1} (light blue bars) for 24 hours. As controls cells treated with DMSO and untreated cells were used. (Data represents media +/- SD of three independent experiments)

The capacity of organotin compound **5** to stain cells at low concentration, at which is not cytotoxic, allows us to propose it as a very good candidate for cell imagining. A deeper study will be necessary in order to stablish its specific subcellular localization, so it can be

used as an organelle specific marker. It would be interesting to analyze the metabolic pathway followed by this compound as it showed a very good cytoplasmic staining but is unable to stain the nucleus. However, even when it seems not to get into the nucleus, at least not the fluorescent forms, it results toxic at several concentrations. It is well-known, that the diorganotin cation moieties binds to DNA, causing cell death by apoptosis,[39] so it would be important to study this mechanism in future experiments. In contrast, compound **3** showed a homogeneous cytoplasmic stain of the cells and worked well at 1 μg mL^{-1}, this pattern suggests not specific organelle staining. Moreover, even at low concentrations remained moderately toxic, which excludes it from live cells experiments. However, it could be an interesting contrast dye to use in fixed cells. There are several contrast dyes for nucleus that are applied on fixed dead cells, as DAPI and Hoechst, in that sense, compound **3** has the potential to be used for cytoplasmic contrast staining. It was unexpected that compound **4** did not stain cells at low concentrations as it was the best at high concentration. Presumably, at low concentrations cells are able to metabolize it, resulting in a non-fluorescent product.

3.6. Bioimaging by Confocal.

To evaluate the applicability of the luminescent organotin compounds as cell imaging agents, confocal fluorescence microscopy measurement was carried out. Cells exposed to either organotin compound at 10 μg mL^{-1} showed different staining patterns ranging from lack of stain to very strong staining (Figure 11). Treatment of cells with compounds **2**, **6**, or **7** did not produce staining (Figure 11C, 11H, and 11I, respectively). Compounds **1** and **8** produce a weak staining (Figure 11C and 11J, respectively). Compound **3** resulted in a strong green homogeneous stain of the cytoplasm (Figure 11E), while compound **4** produced yellow cytoplasmic staining in vesicle-like structures showing stronger staining (Figure 11F). Cells exposed to compound **5** showed a strong cytoplasmic staining produced as well brighter focalized vesicle-like structures (Figures 11G and 11I-K). it is important to notice that no compound is able to stain the nucleus.

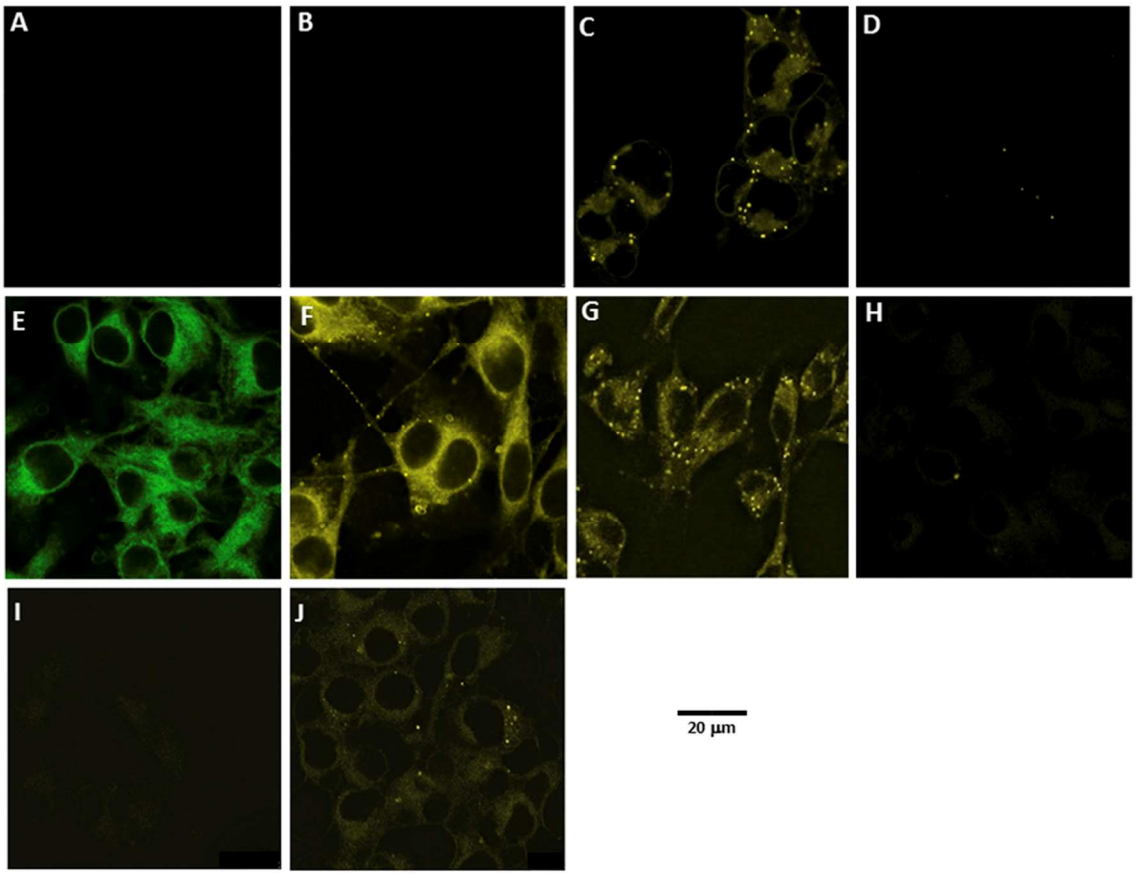

Fig. 11 Staining of cells with organotin compounds. Confocal microscopy of melanoma cells B16F10 treated with 10 μg mL^{-1} of each compound for 2 h. A, Untreated cells; B, DMSO control; C, Compound **1**; D, Compound **2**; E, Compound **3**; F, Compound **4**; G, Compound **5**; H, Compound **6**; I, Compound **7**; J, Compound **8**. (Scale bar shown represents 20 μm).

We sought to analyze the capacity of compounds **3**, **4**, and **5** to stain the cells at lower concentrations. Similar to the previous experiments, B16F10 cells were treated now with 1 mg mL^{-1} or 0.1 mg mL^{-1} of each compound for two hours and then analyzed by confocal microscopy. As shown in Figure 12, compound **3** is able to stain the cells in a dose response way, with strong signal at 10 μg mL^{-1}, moderate at 1 μg mL^{-1} and very weak at 0.1 μg mL^{-1} (Figure 12B, 12C, and 12D, respectively). Compound **5** is able to produce both cytoplasmic and focalized staining even when we lower two magnitude orders its concentration (Figure 12B-D). At 1 μg mL^{-1} produced a staining pattern similar to that at

the higher concentration (Figure 12C), however at the lower concentration of 0.1 μg mL^{-1}, the cytoplasmic staining is almost undetectable but the brighter vesicle-like structures are still visible (Figure 12D). On the other hand, lowering the concentration of compound **4** resulted in a very weak staining at 1 μg mL^{-1} and a complete lack of staining at 0.1 μg mL^{-1} (Figure 12G and 12H, respectively).

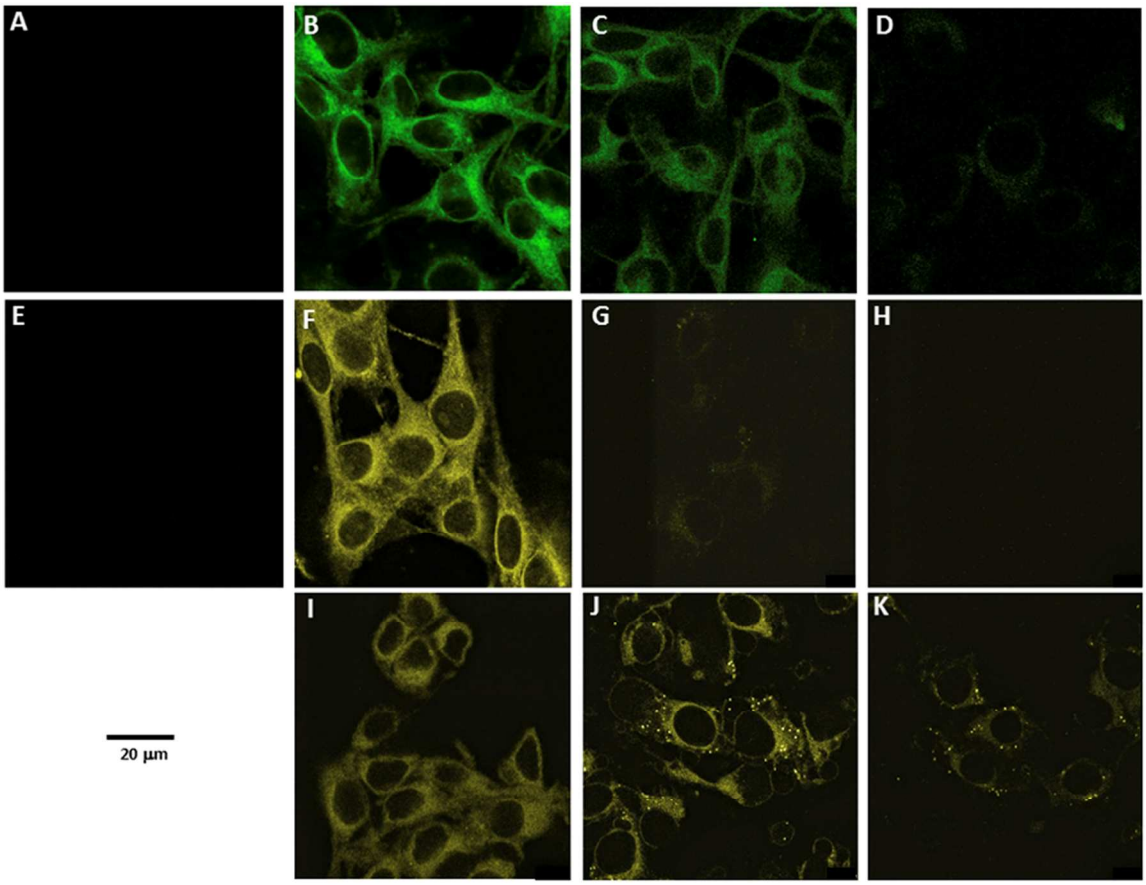

Fig. 12 Staining of cells with organotin compounds **3**, **4**, and **5**. Confocal microscopy of melanoma cells B16F10 treated with compound **3** (B-D), compound **4** (F-H), or compound **5** (I-K) at three different concentrations: 10 μg mL^{-1} (B, F, and I), 1 μg mL^{-1} (C, G, and J), or 0.1 μg mL^{-1} (D, H, and K) of each compound for 2 h. A, Untreated cells; E, DMSO control. (Scale bar shown represents 20 μm).

The very strong yellow cytoplasmic staining in the cells with numerous vesicle-like structures produced by compounds **4** and **5**, suggests that the possible internalization mechanism of the organotin compounds is endocytosis. We hypothesize that after

endosome processing the compound and/or its metabolites are released to the cytosol. Vesicle formation may be influenced by the solubility of the molecule, if not completely solubilized microprecipitates are formed which lead to the internalization of the compound by endosomes. Another possible mechanism is that the compounds are being recognized by cell surface receptors inducing in this way endocytosis. It is important to mention that, high intensity luminescence from the vesicles might be explained on the basis of the acidic internal pH. We infer that the cytosol luminescence is due to the internalization of organotin complex; because the free ligand showed lack of staining under the same condition. Interestingly, none of the compounds is able to get into and stain the nuclei, which suggests the dissociation of the chelating ligand and then producing the intermediate R_2Sn^{2+}.[40] According to the staining pattern, the internalization mechanism for compound **3** could be different to those for compounds **4** and **5**. Cells stained with compound **3** showed a homogeneous cytoplasmic color, without focalized staining, which suggests diffusion through the plasmatic membrane.

There is a group of fluorescence dyes that are commonly used to specifically stain the cell nucleus (DAPI, Hoechst, Acridine Orange, Ethidium Bromide, Propidium Iodide, etc.), while some others stain nucleus and cytoplasm (CyTRAK Orange). These fluorochromes are widely used as nucleus counterstains to give an idea of the cell integrity when components of the cytoplasm are analyzed. However, if nuclear structures are studied, those dyes could interfere. Therefore, fluorochromes that only stain cytoplasm and do not penetrate into the nucleus should be used. To our knowledge, there are not such dyes available. Some authors have tried to use commercial fluorochromes (4MU, DCH, BDECF) to stain the cytoplasm and act as pH indicators.[41] Two of the three used molecules used leaked out of the cells, while the third one was able to remain intracellular for at least two hours, its pH sensibility resulted in a poor stain quality. Such results make these compounds not good choices for cytoplasmic counterstains. More recently some organic compounds have been developed to be used in bioimaging. One of these compounds produced a cytoplasmic stain, however, some nuclear structures were stained as well and the staining depends on molecules aggregation.[42] Our organotin compounds **3** and **5** showed a cytoplasm specific stain pattern on unfixed cells, the stains are stable for several

days and nucleus remained totally unstained. These data make our compounds very good choices for cytoplasm counterstains in studies that involve nuclear structures analysis.

4. Conclusion

In summary, we reported the synthesis and characterization of eight new organotin compounds derived from Schiff bases. The organotin complexes are fluorescent in solution at room temperature where the emission peaks are blue shifted with respect to the corresponding free ligand. Luminescence quantum yields for organotin compounds are always higher than that those corresponding ligands. We also studied the potential of these compounds to be used as fluorescence cytoplasm marker for cell imaging. Compound **5** probed to be a very good candidate for this porpoise as it was able to stain cells at low concentration, with practically no cytotoxicity, while compound **3** could be used as a cytoplasmic contrast fluorescent dye for fixed cells.

Acknowledgments

Financial support and scholarships to M. C. García-López, R. Chan-Navarro, J. C. Berrones and J. A. Serrano from the Consejo Nacional de Ciencia y Teconología (CONACyT, México. Grant 156450) are acknowledged. Thanks are given to Dr. Rosa Santillan for X-ray data collection.

References

1 J. W. Lichtman & J.-A. Conchello, *Nat. Meth.,* 2005, **2**, 910-919.

2 F. L. Thorp-Greenwood, R. G. Balasingham and M. P. Coogan, *J. Organomet. Chem.,* 2012, **714**, 12-21.

3 S. Kim, J. Y. Noh, K. Y. Kim, J. H. Kim, H. K. Kang, S.-W. Nam, S. H. Kim, S. Park, C. Kim and J. Kim, *Inorg. Chem.,* 2012, **51**, 3597-3602.

4 D. Maity and T. Govindaraju, *Eur. J. Inorg. Chem.,* 2011, 5479-5485.

5 (a) M. Suresh, A. K. Mandal, S. Saha, E. Suresh, A. Mandoli, R. D. Liddo, P. P. Parnigotto and A. Das, *Org. Lett.,* 2010, **12**, 5406-5409. (b) D. Ray and P. K. Bharadwaj, *Inorg. Chem.,* 2008, **47**, 2252-2254.

6 P. Wang, J. Liu, X. Lv, Y. Liu, Y. Zhao and W. Guo, *Org. Lett.,* 2012, **14**, 520-523.

7 (a) W.-Q. Geng, H.-P. Zhou, L.-H. Cheng, F.-Y Hao, G.-Y. Xu, F.-X. Zhou, Z.-P. Yu, Z. Zheng, J.-Q. Wang, J.-Y. Wu and Y.-P. Tian, *Polyhedron,* 2012, **31**, 738-745. (b) S. M. Crawford, A. A.-S. Ali, T. S. Cameron and A. Thompson, *Inorg. Chem.,* 2011, **50**, 8207-8213. (c) X.-J. Zhao, Q.-F. Zhang, D.-C. Li, J.-M. Dou and D.-Q. Wang, *J. Organomet. Chem.,* 2010, **695**, 2134-2141. (d) E. López-Torres, A. L. Medina-Castillo, J. F. Fernández-Sánchez and M. A. Mendiola, *J. Organomet. Chem.,* 2010, **695**, 2305-2310. (e) S.-L. Cai, Y. Chen, W.-X. Sun, H. Li, Y. Chen and S.-S. Yuan, *Bioorg. Med. Chem. Lett.,* 2010, **20**, 5649-5652.

8 E. Guzmán-Percástegui, J. G. Alvarado-Rodríguez, J. Cruz-Borbolla, N. Andrade-López, R. A. Vázquez-García, R. N. Nava-Galindo, T. Pandiyan, *Cryst. Growth Des.* 2014, **14**, 3742-3757.

9 (a) Y. Fazaeli, M. M. Amini, E. Najafi, E. Mohajerani, M. Janghouri, A. Jalilian and S. W. Ng, *J. Fluoresc.,* 2012, **22**, 1263-1270. (b) J.-K. Park, W.-S. Kim, G. Otgondemberel, B.-J. Lee, D.-E. Kim and Y.-S. Kwon, *Colloids and Surfaces A: Physicochem. Eng. Aspects,* 2008, **321**, 266-270.

10 A. Endo, M. Ogasawara, A. Takahashi, D. Yokoyama, Y. Kato, and C. Adachi, *Adv. Mat.* 2009, **21**, 4802-4806.

11 (a) H. D. Yin, S. W. Chen, L. W. Li and D. Q. Wang, *Inorg. Chim. Acta,* 2007, **360**, 2215-2223. (b) H. D. Yin and S. W. Chen, *J. Organomet. Chem.,* 2006, **691**, 3103-3108. (c) D. K. Dey, B. Samanta, A. Lycka and L. Dahlenburg, *Z. Naturforsch.,* 2003, **58B**, 336-344.

12 H. D. Yin, J.-C. Cui and Y.-L. Qiao, *Polyhedron,* 2008, **27**, 2157-2166,

13 (a) B. M. Muñoz-Flores, V. M. Jiménez-Pérez, R. Santillán, E. Hernández-Fernández, S. T. López-Cortina and B. I. Kharisov, *J. Chem. Cryst.,* 2012, **42**, 34-37. (b) V. M. Jiménez-Pérez, B. M. Muñoz-Flores, H. W. Roesky, T. Schulz, A. Pal, T. Beck, Z. Yang, D. Stalke, R. Santillán and M. Witt, *Eur. J. Inorg. Chem.,* 2008, 2238-2243.

14 M. Ibarra-Rodríguez, H. V. Rasika Dias, V M. Jiménez-Pérez, B. Muñoz-Flores, A Flores-Parra and S Sánchez, *Z. Anorg. Allg. Chem.,* 2012, **638**, 1486-1490.

15 V. M. Jiménez-Pérez, M. Ibarra-Rodríguez, B. M. Muñoz-Flores, A. Gómez, R. Santillán, E. Hernández-Fernández, S. Bernès, N. Waksman and R. Ramírez, *J. Mol. Struct.,* 2013, **1031**, 168-174.

16 V. M. Jiménez-Pérez, B. M. Muñoz-Flores, L. M. Blanco Jerez, A. Gómez, L. D. Rangel, R. Chan-Navarro, N. Waksman and R. Ramírez-Durón, *Int. J. Electrochem. Sci.* 2014, **9**, 7431-7445

17 The Manipulation of Air-Sensitive Compounds, by Duward F. Shriver and M. A. Drezdzon 1986, J. Wiley and Sons: New York.

18 G. M. Sheldrick, *Acta Crystallogr. Sect. A* 1990, **46**, 467-473.

19 G. M. Sheldrick, *SHELX-97*: Program for the Solution and Refinement of Crystal Structures; Universität Göttingen: Göttingen, Germany, 1997

20 L. J. Farrugia, *J. Appl. Crystallogr.,* 1999, **32**, 837-838.

21 A. Felouat, A. D'Aléo and F. Fages, *J. Org. Chem.* 2013, **78**, 446−4455.

22 A. T. R. Williams, S. A. Winfield and J. N. Miller, *Analyst,* 1983, **108**, 1067-1071.

23 S. A. El-Daly, S. A. El-Azim, F. M. Elmekawey, B.Y. Elbaradei, S. A. Shama and A. M. Siri, *Int. J. Photoenergy*, 2012, **2012**, 1-10.

24 J. Holecek, M. Nadvornik, K. Handlir and A. Lycka, *J. Organomet. Chem.,* 1986, **315**, 299-308.

25 D. Dakternieks, A. Duthie, D. R. Smyth, C. P. D. Stapleton and E. R. T. Tiekink, *Organometallics,* 2003, **22**, 4599-4603.

26 F. P. Pruchnik, M. Banbula, Z. Ciunik, M. Latocha, B. Skop, T. Wilczok, *Inorg. Chim. Acta,* 2003, **356**, 62-68.

27 B. Wrackmeyer, NMR spectroscopy of tin chemistry, in: A.G. Davies, M. Gielen, K. H. Pannell, E. R. T. Tiekink (Eds.), Tin Chemistry: Fundamentals, Frontiers and Applications, John Wiley & Sons, United Kingdom, 2008.

28 J. Holeček, M. Nádvorník, K. Handlíř, *J. Organomet. Chem.* 1986, **315**, 299-308.

29 H. I. Beltrán, L. S. Zamudio-Rivera, T. Mancilla, R. Santillán and N. Farfán, *Chem. Eur. J.* 2003, **9**, 2291-2306.

30 N. Kobakhidze, N. Farfán, M. Romero, J. M. Méndez-Stivalet, M. G. Ballinas-López, H. García-Ortega, O. Domínguez, R. Santillán, F. Sánchez-Bartez and I. Gracia-Mora, *J. Organomet. Chem.,* 2010, **695**, 1189-1199.

31 F. E. Smith, R. C. Hynes, T. T. Ang, L.E. Khoo and G. Eng, *Can. J. Chem.,* 1992, **70**, 1114–1120.

32 K. M. Chow and K. M. Lo, *Polyhedron,* 2014, **81**, 370-381.

33 H. D. Yin and S. W. Chen, *J. Organomet. Chem.,* 2006, **691**, 3103-3110.

34 R. Chan-Navarro, V. M. Jiménez-Pérez, B. M. Muñoz-Flores, H. V. Rasika Dias, I. Moggio, E. Arias, G. Ramos-Ortíz, R. Santillán, C. García, M. E. Ochoa, M. Yousufuddin and N. Waksman, *Dyes and Pigm.* 2013, **99**, 1036-1043.

35 M. C. García-López, B. M. Muñoz-Flores, V. M. Jiménez-Pérez, I. Moggio, E. Arias, R. Chan-Navarro and R. Santillán, *Dyes and Pigm.* 2014, **106**, 188-196.

36 J. R. Lakowicz, Principles of Fluorescence Spectroscopy, 2nd ed. Kluwer Acc. Press (1999) New York.

37 a) S.-H. Li, F. R. Chen, Y. F. Zhou, J. N. Wang, H. Zhang and J. G. Xu, *Chem. Commun.* 2009, 4179. b) S.-L. Cai, Y. Chen, W.-X. Sun, H. Li, Y. Chen, S.-S. Yuan, *Bioorg. Med. Chem. Lett.* 2010, **20**, 5649-5652.

38 E. C. Glazer, D. Magde, and Y. Tor, *J. Am. Chem. Soc.* 2007, **129**, 8544-8551.

39 (a) L. Pellerito and L. Nagy, *Coord. Chem. Rev*., 2002, **224**, 111–150 and references therein; (b) M. L. Falcioni, M. Pellei and R. Gabbianelli, *Mutat. Res.,* 2008, **653**, 57–62 and references therein; (c) Q. Li, P. Yang, H. Wang and M. Guo, *J. Inorg. Biochem.,* 1996, **64**, 181–195.

40 (a) J. S. Casas, E. E. Castellano, M. D. Couce, J. Ellena, A. Sánchez, J. L. Sánchez, J. Sordo and C. Taboada, *Inorg. Chem.,* 2004, **43**, 1957–1963; (b) Y. Arakawa, *Biomed. Res. Trace Elem.,* 2000, **11**, 259–286.

41 E. Musgrove, C. Rugg, and D. Hedley. *Cytometry* 1986, **7**, 347-355.

42 Y. Liu, M. Kong, Q. Zhang, Z. Zhang, H. Zhou, S. Zhang, S. Li, J. Wu and Y. Tian, *J. Mater. Chem. B*, 2014, **2**, 5430-5440.

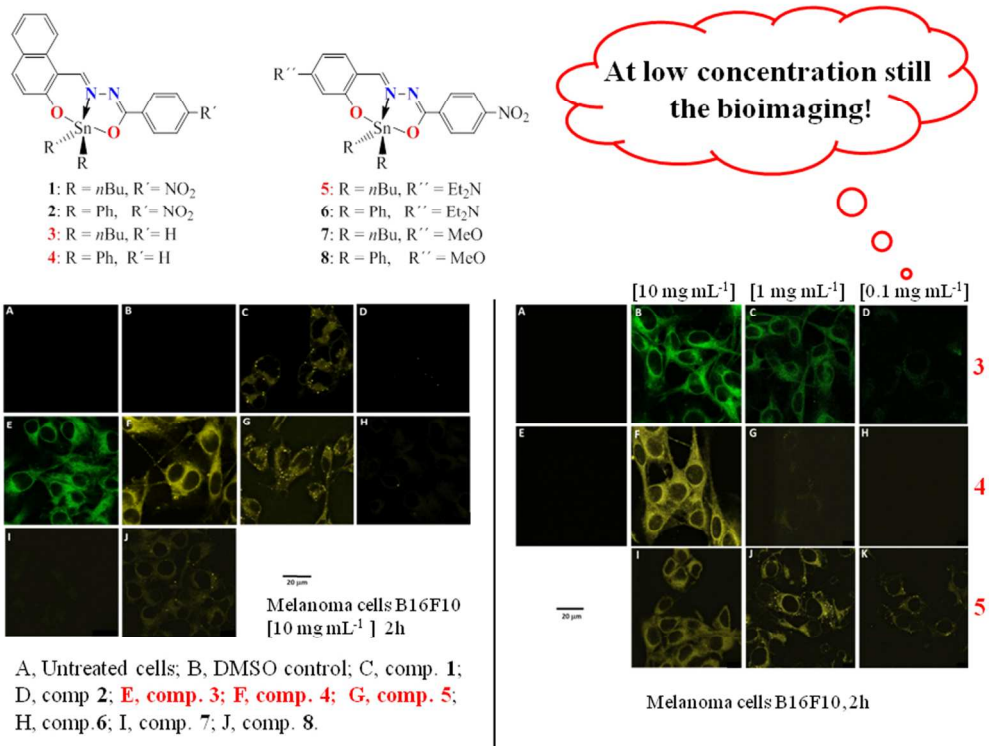

A novel application of fluorescent organotin compounds derived from Schiff bases were developed for imaging cells.
254x190mm (96 x 96 DPI)